Master of Science conjoint HES-SO - UNIL en Sciences de la santé
Av. de Provence 6
CH-1007 Lausanne

Master of Science conjoint HES-SO - UNIL en Sciences de la santé

Orientation Technique en radiologie médicale

Comparing dynamic susceptibility contrast perfusion post-processing with different clinically available software among patients affected of a high-grade glioma.

Fait par

Eloïse Delacoste

Sous la direction de
Bénédicte Delattre, Ph.D, physicienne
Prof. Maria Isabel Vargas, M.D., responsable de l'unité de neuroradiologie diagnostique et du secteur IRM
De l'institution des Hôpitaux Universitaires de Genève

Expert : Prof. Jean-Noël Hyacinthe, Ph.D., physicien et professeur à la HES-SO//Master
Président du Jury : Prof. Jean-Noël Hyacinthe, Ph.D., physicien et professeur à la HES-SO//Master

Genève, HES-SO//Master, 2018

Accepté par la HES-SO//Master (Suisse, Lausanne) sur proposition de

Prof. Jean-Noël Hyacinthe, président du Jury

Lausanne, le 23 décembre 2018

Prof. Olivier Contal
Responsable du module
Travail de Master

Prof. Ludivine Soguel Alexander
Responsable de la filière MScSa

“I was taught that the way of progress was neither swift nor easy.”

Marie Curie, 1923

Acknowledgements

Several people supported me and contribute to the realization of this master's work. I would like to warmly thank everyone personally, especially to:

Madam Delattre, the director of this master's work, whom followed and supported me throughout the year, always available to help me find solutions and give me tips.

Dre Vargas, the co-director of this study, whom supported me and provided the data needed but also trained us and controlled the post-processing.

Mr. Hyacinthe, the president of the jury and the expert, whom offered me his help to define the subject of study.

Dr Wanyanga, internal doctor in oncology, whom was the second operator of this study and whom gave his time to carry out the post-processing of the whole sample on Olea Sphere.

Madam Doutaz-Meyer, as well as all the executives of X-Ray SA, whom allowed me to study many hours on my Mastership and facilitated me to realize it.

Finally, my last but not least thank goes to my family and friends whom helped me with the work's correction, but mostly for supporting me all year long.

Abbreviations

AIF	Arterial Input Function
ASFNR	American Society of Functional Neuroradiology
BBB	Blood-Brain Barrier
CBF	Cerebral Blood Flow
CBV	Cerebral Blood Volume
DCE	Dynamic Contrast-Enhancement
DSC	Dynamic Susceptibility Contrast
DTI	Diffusion Tensor Imaging
EPI	Echo Planar Imaging
GE	Gradient Echo
HUG	Geneva University Hospitals
ICC	Intraclass Correlation Coefficient
MRI	Magnetic Resonance Imaging
MTT	Mean Time Transit
nrCBV	normalised relative Cerebral Blood Volume
rBV	relative Blood Volume
rBVcorr	relative Blood Volume corrected
rCBV	relative Cerebral Blood Volume
ROI	Region of Interest
SD	Standard Deviation
WHO	World Health Organization (OMS in french)

Abstract in french

Objectif

L'objectif principal de cette étude rétrospective était d'évaluer la variabilité inter-logicielle lors du post-traitement d'une perfusion T2* à l'IRM provenant de patients atteints d'un gliome de haut grade.

Matériel et méthode

Les patients inclus étaient atteints soit d'un astrocytome anaplasique (OMS grade III), soit d'un glioblastome (OMS grade IV) situé dans le parenchyme cérébral. Le post-traitement de 54 perfusions T2* provenant de 46 patients, a été réalisé en utilisant les logiciels Intellispace© (Philips) et Olea© (Olea Medical). Le paramètre hémodynamique étudié était le volume sanguin cérébral relatif corrigé de l'effet de fuite T1 (rCBV) avec une référence controlatérale. La variabilité inter-opérateur sur Olea et la variabilité entre les méthodes proposées par Intellispace ont également été évaluées.

Résultats

Concernant la reproductibilité inter-logicielle, l'ICC et le Kappa de Cohen pour le suivi thérapeutique obtenu étaient de 0.74 et 0.61, proches des limites recommandées de 0.75 et 0.60 respectivement. Des sous-groupes ont été créés pour compléter l'analyse. Même si la nécrose ou les structures vascularisées ont été éliminées des ROI, les résultats ne se sont pas améliorés. Des régions d'intérêt avec une aire minimum de 250mm^2 ont atteint un ICC et un Kappa de Cohen au-dessus du seuil. La reproductibilité inter-opérateur sur Olea et la reproductibilité sur Intellispace étaient satisfaisantes pour une hypothèse clinique valide.

Conclusion

La reproductibilité entre Intellispace et Olea n'était pas idéale pour un contexte clinique. Cette divergence peut s'expliquer par l'effet de volume partiel, d'une différence dans les modèles utilisés et la manière de l'implémenter dans le logiciel. Des ROI avec une aire de minimum 250mm^2 améliore cette variabilité afin qu'elle devienne acceptable.

Mots-clés

Perfusion cérébrale T2*, IRM, EG, glioblastome, astrocytome, Intellispace Portal, Olea Sphere, correction de fuite, fonction gamma, variabilité inter-logicielle, variabilité inter-opérateur, variabilité intra-logicielle

Abstract

Objective

The main purpose of this retrospective study was to evaluate inter-software variability in patients affected of a high-grade glioma for the post-processing of dynamic susceptibility contrast (DSC) perfusion imaging in MRI.

Materials and methods

The included patients were either anaplastic astrocytoma (WHO grade III) or glioblastoma (WHO grade IV) located in the cerebral parenchyma. The post-processing of 54 DSC-MRI from 46 patients using both Intellispace© (Philips) and Olea© (Olea Medical) software was performed. The hemodynamic parameter studied was the relative cerebral blood volume corrected for the T1 leakage effect (rCBV) with a contralateral reference. The inter-operator variability within Olea and the variability between the methods proposed in Intellispace were also evaluated.

Results

Regarding inter-software reproducibility, ICC and Cohen's Kappa from therapeutic follow-up obtained were 0.74 and 0.61, close to the recommended limits of 0.75 and 0.60 respectively. Subgroups were created to complete the analysis and to evaluate the partial volume effect. Even if necrosis or vascular structures from regions of interest (ROI) were avoided, results did not improve. ROI of a minimum area of 250mm^2 yielded an ICC and Cohen's Kappa above the threshold. The inter-operator reproducibility on Olea and intra-software reproducibility on Intellispace were satisfactory for a clinical valid assumption.

Conclusion

The reproducibility between Intellispace and Olea was not ideal for a clinical context. This discrepancy can be explained by the partial volume effect and a difference in the models used and how to implement it in the software. ROI with an area of at least 250mm^2 improves this variability and becomes acceptable.

Keywords

DSC, cerebral perfusion, imaging, MRI, GE, T2*, glioblastoma, astrocytoma, Intellispace Portal, Olea Sphere, leakage correction, gamma variate, inter-software variability, inter-operator variability, intra-software variability

Contents

1. Introduction 11

2. State of the art 12
2.1 Leakage effect 12
2.2 Leakage correction 12
2.2.1 Dual-echo pulse sequence 12
2.2.2 Preload dose 12
2.2.3 Other contrast agent 13
2.2.4 Leakage-corrected post-processing 13
2.3 Clinical application 14
2.4 Diagnostic 14
2.5 ASFNR Recommendations 15

3. Research goal 16

4. Materials and methods 17
4.1 Ethic 17
4.2 Operators 17
4.3 Patients 17
4.4 Acquisition 18
4.5 Post-processing software 18
4.5.1 Intellispace 19
4.5.1.1 Manual AIF 19
4.5.1.2 Model free 19
4.5.1.3 Gamma variate 19
4.5.1.4 Leakage correction 20
4.5.2 Olea 20
4.5.2.1 Arterial Input Function (AIF) 20
4.5.2.2 Deconvolution 21
4.5.2.3 Leakage correction 21
4.6 Region of Interest (ROI) 21

4.7 Inter-software reproducibility 22
4.7.1 Leakage correction 22
4.7.2 Adjacent tissue influence 22
4.7.3 Size ROI influence 23
4.7.4 Tumour influence 23
4.8 Inter-operator reproducibility on Olea 23
4.9 Intra-software reproducibility on Intellispace 23
4.10 Statistical methods 23

5. Results 25
5.1 Inter-software reproducibility 25
5.1.1 rCBV reproducibility between Intellispace and Olea 25
5.1.2 Adjacent tissue influence 27
5.1.3 Size ROI influence 28
5.1.4 rCBV's healthy structure 29
5.1.5 Visual assessment of rCBV 30
5.2 Inter-operator reproducibility on Olea 32
5.2.1 rCBV reproducibility between two operators 32
5.2.2 Visual assessment of rCBV 33
5.3 Intra-software reproducibility on Intellispace 35
5.3.1 rCBV reproducibility between leakage correction and gamma variate 35
5.3.2 Visual assessment of rCBV 36
5.4 Summary table of results 38

6. Discussion 38
6.1 Inter-software reproducibility 38
6.2 Inter-operator reproducibility on Olea 39
6.3 Intra-software reproducibility on Intellispace 40
6.4 Limitations 40
6.4.1 Intra-operator variability 40
6.4.2 Sample size 40
6.5 Perspectives 41

7. Conclusions and recommendation 42
7.1 Inter-software reproducibility 42
7.2 Inter-operator reproducibility on Olea 42
7.3 Intra-software reproducibility on Intellispace 43

Summary in french – Résumé en français 44
Introduction 44
Problématiques 44
Matériel et méthode 44
Résultats 45
Discussion 46
Conclusions et recommandation 46

References 47
Bibliography 53

Content of the exhibit 58
Content of the tables 59

1. Introduction

Brain imaging provides the physiological and functional information needed to visualize and evaluate the entire brain, the main organ of the central nervous system. One of the principal physiological processes to be analysed is cerebral perfusion, which quantifies vascularization and angiogenesis. For this, several radiological methods can obtain the same information, but each has its own benefits and limitations.

Dynamic Susceptibility Contrast (DSC) perfusion imaging by Magnetic Resonance Imaging (MRI) is one of the most used techniques in the clinic to quantify cerebral perfusion. This method involves injecting an exogenous paramagnetic contrast agent during a T2-weighted ultra-fast sequence. The first pass of a fast bolus of gadolinium will induce a loss of intensity of the T2* signal. Thanks to Østergaard's model of Leif Østergaard, it is possible to deduce important hemodynamic parameters such as Cerebral Blood Flow (CBF), Cerebral Blood Volume (CBV) or Mean Transit Time (MTT) among others (Østergaard et al., 1996). To obtain accurate quantitative results, the model requires knowing the Arterial Input Function (AIF). In the absence of a precise AIF, the hemodynamic parameters are relative, semi-quantitative. Therefore, it is necessary to normalise the results obtained from the lesion with a contralateral normal-appearing tissue.

The two principal indications of a DSC-MRI are brain tumours and stroke. The parameter mainly evaluated is not the same according to the indication. In the context of a brain tumour, the essential hemodynamic parameter for tumour assessment and follow-up is relative Cerebral Blood Volume (rCBV).

Among brain tumours, glioma is the most common primary neoplasm. It is divided into three categories according to the classification of the World Health Organization (WHO, 2016): oligoastrocytoma, oligodendroglioma and astrocytoma. Statistics regarding patient survival differ by glioma type, grade and treatment. Anaplastic astrocytoma (WHO grade III) has a median survival around three years. While a patient with a glioblastoma multiforme (WHO grade IV) has a median survival of twelve to eighteen months (Dong et al., 2015). Angiogenesis, the process of forming new vessels, is one of the characteristics of aggressive tumours.

2. State of the art

2.1 Leakage effect

In a DSC-MRI perfusion, the first-pass of gadolinium is analysed with the dilution indicator theory. This is based on the principle that the contrast agent is confined to the intravascular space by the blood-brain barrier (BBB). When this is leaky, which is the case during brain tumour, the contrast agent extravasates into the extracellular extravascular space, which alters the quantification of hemodynamic parameters by modifying the post-bolus signal. This contrast leakage effect is explained by a complex and multifactorial interaction between T1- and T2*-weighting that may overestimate or underestimate rCBV as a function of the predominance of weighting. In case of predominance of T1-weighting, the post-bolus signal overshoots the baseline, which underestimates the rCBV. Whereas in case of predominance T2*, the post-bolus signal does not reach the baseline pre-bolus, which overestimates the rCBV.

2.2 Leakage correction

The leakage effect caused by a blood-brain barrier breakdown is more marked in high-grade tumours because vascular permeability is high. Therefore, when evaluating a glioma, it is important to mitigate this negative effect to obtain corrected relative cerebral blood volume. For this, there are four main methods that correct the signal of the post-bolus baseline.

2.2.1 Dual-echo pulse sequence

The first method is to modify the DSC perfusion sequence. It consists in using two different TE with the same principle as inversion recovery images during the bolus. With this type of pulse sequence, it is theoretically possible to remove the T1 contribution of the acquired signal. This technique is used in some studies (Vonken & Viergever, 1999), (Paulson & Schmainda, 2008), (Pickens, Price, & Yankeelov, 2012) and is recognized to give results in agreement with other methods.

2.2.2 Preload dose

The second method is to inject a preload dose before the gadolinium dose required for DSC-MRI; the patient is injected twice during the examination. It will allow to saturate the extracellular extravascular space to reduce the signal from this region during the second

injection. It is possible to inject the same amount of preload as during the examination (1 + 1) or to inject less preload (<1 + 1). Several studies (Paulson & Schmainda, 2008), (Hu et al., 2010), (Boxerman et al., 2012), (Leu, Boxerman, & Ellingson, 2017) have evaluated the effectiveness of this method and conclude that the rCBV ratio estimation is more accurate. T1-weighted imaging is usually performed during the first injection to use as a scout for the slice positioning of the subsequent injection.

2.2.3 Other contrast agent

Regarding the injection of the bolus, it is also possible to change the contrast agent during the DSC-MRI. Indeed, some other contrast agents do not cross the vascular barrier even with a broken BBB. Some research (Christen et al., 2013), (Gahramanov et al., 2013) has investigated different contrast agents such as ferumoxytol which is a blood pool agent providing hemodynamic parameters like rCBV. These studies conclude that ferumoxytol provides better tumour monitoring than gadolinium-based contrast agents and does not require a leakage correction.

2.2.4 Leakage-corrected post-processing

The last technique is the one examined during this study. The principle of this method is to virtually eliminate the effect of leakage caused by the BBB breakdown after the acquisition, in post-processing using an algorithm. For this, many mathematical models have been created and studied since several decades.

In 1964, Thompson et al. have suggested that the concentration curve has the same properties as a gamma function (Thompson, Starmer, Whalen, & Mcintosh, 1964). Since then, several studies have evaluated and approved the efficiency to the fit of the curve acquired with a DSC-MRI to a gamma variate function (Davenport, 1983), (Benner et al., 1997), (Law et al., 2004). Therefore, this mathematical function has been added in some post-processing software used clinically.

It is only in 2006 that Jerrold L. Boxerman and Robert M. Weisskoff proposed a complex mathematical model (Boxerman, Schmainda, & Weisskoff, 2006). The hemodynamic parameters are corrected by removing the leakage term, which allow to generate an estimate of the permeability. It has been shown by other studies that this algorithm is robust enough to not require a precise pattern of imaging sequence or contrast injection (Bjornerud, Sorensen, Mouridsen, & Emblem, 2011), (Boxerman et al., 2012).

Clinically available post-treatment software offer several post-processing methods that are relatively well explained in their user manual. However, software makers, due to copyright may not always deliver precise information about the exact implementation of the model fitting.

2.3 Clinical application

Numerous clinical applications are available for brain tumours, but also for gliomas in particular, thanks to rCBV obtained by T2*-weighted DSC-MRI perfusion. In general, an increase in rCBV suggests a process of neoangiogenesis (Donahue et al., 2000).

In first place, DSC perfusion imaging allows to differentiate low-grade glioma with low rCBV from high-grade glioma with high rCBV (Law et al., 2004), (Emblem et al., 2008) and provides the predicted time to tumour progression (Hirai et al., 2008), (Law et al., 2008). In addition, it can target a biopsy (Maia et al., 2004) to the higher-grade region or offer a per-operative guide (Ulmer et al., 2009).

Secondly, the patient's treatment can also be evaluated to distinguish a pseudo-progression from a pseudo-regression (Hu et al., 2009) during a chemoradiotherapy treatment. If the treatment is effective a decrease in rCBV is noticeable. In stereotactic radiotherapy, DSC allows to differentiate radionecrosis with low rCBV from tumour recurrence with high rCBV (Barajas et al., 2009). Finally, during an antiangiogenic therapy, it is possible to differentiate a tumour response with a low rCBV against a pseudo-response with a high rCBV (Essock-Burns et al., 2011).

2.4 Diagnostic

The rCBV ratio obtained from the DSC perfusion is the result of the rCBV division of the lesion by the rCBV of the healthy tissue reference. There is a cohesion in the literature on how to calculate this rCBV ratio, but some of these studies differ on where the cut-off point should be set. Indeed, according to each indication the minimum threshold of the ratio rCBV varies (Bulakbasi et al., 2005). Concerning angiogenesis, Al-Okaili et al. determine a fixed cut-off at 1.75 of rCBV ratio (Al-Okaili et al., 2006). Beyond this threshold, the proliferation of new vessels can be considered significant. While Jenoudet et al. advise a range of the rCBV ratio of 1.5 to 2 instead of 1.75 (Jenoudet et al., 2007).

2.5 ASFNR Recommendations

The American Society of Functional Neuroradiology (ASFNR) provided in 2016, recommendations for DSC-MRI perfusion (Welker et al., 2015). For this, a review of current studies was conducted to provide advice on clinical applications, examination parameters, post-processing, interpretation of results and reports. However, these recommendations are a review of typical uses without precise guideline. To begin, in that report there is an acronym "nrCBV", which is the rCBV normalised by a contralateral healthy region. In this present study, the nrCBV is the rCBV ratio.

There is no DSC-MRI sequence common to all studies with the same parameters (TE, TR, flip angle). They are interdependent and vary with each other depending on the strength of the field and the site preferences. It is a trade-off between the desired signal-to-noise ratio and the acceptable T1 sensitivity for the extravasation of the contrast agent.

The ASFNR recognizes the benefits of using a Dynamic Contrast-Enhanced (DCE) perfusion sequence that can complements the information obtained by a DSC for tumour evaluation. These two perfusions can be performed during a single examination with two injections. The DCE is carried out before the DSC to serve as a preload dose.

Regarding the post-processing, the fitting to a gamma variate function is generally not advisable because it is inherently noisy. Instead, it is recommended to use a model that adjusts the acquired curve and generates an estimate of the permeability. According to the studies, preload with an incubation time of 5 to 10 minutes, coupled with a leakage-corrected post-processing is one of the methods to better distinguish the hemodynamic parameters of a tumour with a contrast leakage effect.

The ASFNR wants to point-out that the cut-off thresholds used may vary according to the acquisition, injection and post-processing patterns. The report does not provide a minimum threshold according to the indications.

3. Research goal

The main research goal of this study is to determine if the results obtained between two different software, Intellispace Portal and Olea Sphere, are consistent for DSC leakage-corrected post-processing. Indeed, numerous post-processing software are on the market, so it is important that the clinical opinion resulting from the analysis of the DSC is similar. This study took place within the Geneva University Hospitals (HUG), as several post-processing software are available; they are of course directly affected by this issue, like in many other medical institutions.

The second aim is to analyse the reproducibility between two operators on Olea Sphere. This allows to determine if inter-operator variability is acceptable. In fact, in a clinical context, it is important that one particular software always provides the same result even if it is not the same operator who performs the analysis. At HUG, there is not an assigned person to the DSC post-processing. It is the role of residents doctors in radiology whom may change their affectation to another service. Human variability therefore exists, although post-processing is controlled by a clinical professor.

The last problematic of this study aims at determining if the gamma variate method is comparable to the algorithm of Boxerman-Weisskoff on Intellispace Portal. Indeed, as noted above, the ASFNR since 2016 no longer recommends the use of gamma variate. Before then, it was advisable to carry out post-processing in this way, so it is newly important that the clinical opinion arising from gamma variate always corresponds to the new algorithm.

4. Materials and methods

4.1 Ethic

This retrospective study was approved by the Geneva Cantonal Commission for Ethics of Scientific Research (CCER). The project was number 2016-01821 and informed consent was waived.

4.2 Operators

In order to be able to evaluate the inter-operator reproducibility within the same software, at least two operators are needed. The second operator in this study was Dr Wanyanga, junior in oncology at the Freiburg Hospital with one year of experience. Both of us have been trained by Prof MI Vargas, senior neuroradiologist with 22 years of experience, whom has also frequently checked the accuracy of our post-processing. The data collection lasted several months during the year 2018, from March to November.

4.3 Patients

Data from 46 patients initially diagnosed with a primary brain tumour were retrospectively collected for their treatment. They were all treated by radiotherapy or stereotactic radiosurgery between January 1st, 2014 and December 31st, 2016 in the Geneva University Hospitals.

The inclusion criteria were either anaplastic astrocytoma (WHO grade III) or glioblastoma (WHO grade IV) in the cerebral parenchyma, tumour enhancement in post-gadolinium T1-weighted imaging, but also the delay between surgery or biopsy and DSC. Indeed, one or two MRI exams were chosen for each patient; the first before radiotherapy that was previous to the biopsy or surgery and the second at least three months after the end of radiation treatment. This leaves time for radiation necrosis to appear which does at least three months after radiotherapy.

The exclusion criteria were the presence of another pathology, as well as the quality of images such as motion artefacts.

On a baseline sample of 46 patients and 72 examinations, 18 DSC were excluded mainly because of the nature of the tumour, its location, as well as the image quality. The final sample

of this study includes 54 examinations belonging to 35 patients (ratio M/F: 2.19:1, average age: 59 years old [min: 27, max: 73]).

4.4 Acquisition

All acquired images come from two different 3T MRIs systems (Skyra or Prisma Fit from Siemens, Erlangen, Germany). The sequences used are part of the clinical HUG brain tumour protocol. It includes T1, T2 and 3DFLAIR anatomical sequences with diffusion tensor imaging (DTI). After performing these sequences, the contrast bolus can be started a few seconds after the EPI GE T2* acquisition used for DSC-MRI (TE=27-35ms, TR=1.5-1.6s, flip angle=60/75/90°). Once the DSC is complete, a post-gadolinium 3D T1-weighted sequence is performed. This last acquisition is the one showing the tumour enhancement.

The contrast agent used at HUG is Gadovist (Bayer Schering Pharma, Berling-Wedding, Germany) with 0.1 mmol/kg of the patient without preload. The injections are all performed using an automatic injector with a flow rate of 5 cc/s and they are each followed by 20 ml of physiological solution at the same rate.

4.5 Post-processing software

Several software packages are available at the HUG to perform post-processing of DSC imaging. However, they will not all be evaluated during this project. The two programs studied are able correcting the leakage of gadolinium-based contrast agent effect caused by the blood-brain barrier breakdown.

- Intellispace Portal version 9.0 (Philips Healthcare, Best, Netherlands)
- Olea Sphere version 3.0 – SP6 (Olea Medical, Cambridge, Massachusetts, USA)

For simplification, Intellispace Portal will be abbreviated Intellispace and Olea Sphere by Olea.

The first software package was created by X-ray manufacturers, while the latest Olea Sphere was developed by independents and bought by Toshiba Medical (Tokyo, Japan) then by Canon Medical Systems Corporation (Tokyo, Japan). However, both software have been approved by the US Food and Drug Administration (FDA, 2016).

4.5.1 Intellispace

The radiological device manufacturer Philips has released the Intellispace post-processing software. The latter has many possibilities including the DSC's analysis. Version 9.0 of this software, available since 2017, has four different methods to quantify the cerebrovascular's parameters.

4.5.1.1 Manual AIF

The first and most basic method requires the operator to select the arterial input function, usually on a Willis polygon artery contralateral to the brain injury. The software will then perform a deconvolution with the AIF and the acquired signal, to be able to calculate the different cerebrovascular parameters such as the cerebral blood volume thanks to the Østergaard model (Østergaard et al., 1996).

4.5.1.2 Model free

This method uses an automatic AIF selected by the software. It detects the beginning and the end of the bolus on the acquired curve. The baseline before and after the peak is detected in order to be able to fit the curve and thus highlight the various parameters specific to the DSC (fig. 1).

4.5.1.3 Gamma variate

Intellispace also offers a method of gamma variate, recommended in the past literature (Law et al., 2004). This is based on the principle that the flow's ideal form of the contrast agent is comparable to a gamma function. The software will thus fit the perfusion curve acquired with the gamma function (fig. 2). Therefore, this technique makes it possible to reduce the effects associated with the contrast agent's leakage and on the second pass' effect.

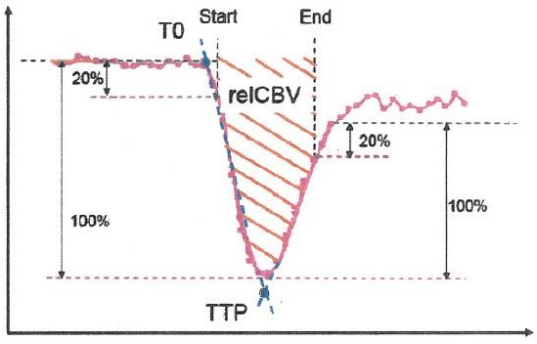

Figure 1: Model free on Intellispace (source: MR Neuro Perfusion in ISP9)

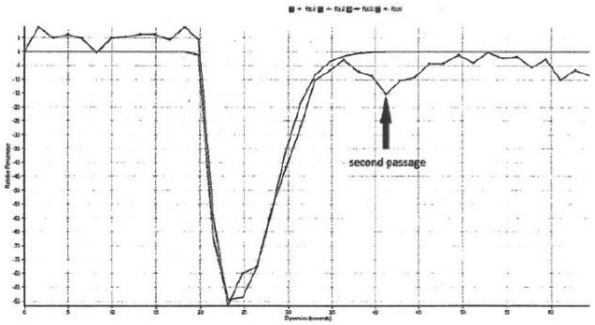

Figure 2: Model free on Intellispace (source: MR Neuro Perfusion in ISP9)

4.5.1.4 Leakage correction

This method is available only from version 9.0 It is a leakage-corrected post-processing that quantifies a negative T1- or T2-weighted effect on the acquired curve, thanks to the Boxerman-Weisskoff model (Boxerman et al., 2006). This model has two compartments (fig. 3). For this, it will create, from all the voxels of the acquisition, a first compartments that models the nadir and the second that models the leakage effect. The acquired perfusion curve will then be compared with these two models and to allow this adjustment's parameters (K1 and K2). The K1 has no unit of measure, while the K2 values are in 10^{-3}/min.

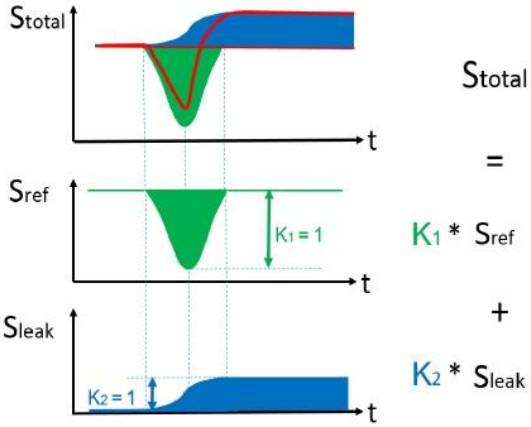

Figure 3: Leakage correction on Intellispace (source: MR Neuro Perfusion Leakage correction)

4.5.2 Olea

The second post-processing software presented is Olea. This one, unlike Intellispace was designed by independents and was later bought by X-ray manufacturers. It also has numerous post-processing possibilities such as an evaluation of DSC-MRI.

The Olea software is a little different from Intellispace. In fact, at start, Olea does not present the different methods such as a mandatory decision to take in order to generate the cerebrovascular maps. It does it otherwise, it divides the work into two stages: first generating the maps and second by analysing them with the placement of the ROI. Of course, some options and corrections are activated. It is however possible to modify almost all of them.

4.5.2.1 Arterial Input Function (AIF)

Regarding the Olea software, just like Intellispace, it is as well possible to define the AIF itself by selecting a voxel in an artery. The perfusion curve acquired of this unique voxel will then be the reference of the arterial input function necessary to achieve the deconvolution.

If the operator doesn't select this option, Olea automatically defines the input arterial function. Actually, several voxels with a high perfusion are selected and then averaged to get the AIF. Even though some voxels automatically selected by Olea are not in an artery but on an intense hyposignal, the curve is the average of the signal intensity of all selected voxels, which can thus be reliable.

4.5.2.2 Deconvolution

Then, the operator may define the singular value of the deconvolution method that Olea uses (standard [sSVD], block-circulating [cSVD] or oscillation index [oSVD]). According to the documents accompanying Olea (Olea Medical, 2013), the method with the most stable and accurate estimates, as well as the best predictive potential among the different types of deconvolution is the oSVD method with oscillation index.

4.5.2.3 Leakage correction

In addition to the deconvolution technique and the choice of the AIF, the operator can activate a software option, allowing Olea to consider the effects caused by contrast agent's leakage across the blood-brain barrier. This will correct the rCBV, the area under the curve by the following formula from Boxerman-Weisskoff model (Boxerman, Schmainda, Weisskoff, 2006):

$$rBVcorr = rBV + K2 \int_0^T dt'' \int_0^{t''} \Delta R2 * (mean)(t')(dt')$$

For this, the leakage factor K2 (varying according to the pixel) and the time $\int_0^T dt'' \int_0^{t''} \Delta R2 * (mean)(t')(dt')$ (identical for all dataset) is added to the uncorrected relative blood volume (rBV) in order to obtain the corrected relative blood volume (rBVcorr). Unlike Intellispace, the Olea K2 does not have a unit of measure.

4.6 Region of Interest (ROI)

After generating the cerebral blood volume map, it is necessary to place the regions of interest to semi-quantitatively evaluate the glioma. For that purpose, the tumour ROI was positioned to cover the hyperperfused zone on the post-gadolinium T1-weighted imaging in agreement with the generated map of K2. As a matter of fact, the parameter K2 allows to reveal the regions affected by the leakage effect. Knowing that necrosis is typically present in glioblastomas, it is difficult to avoid it completely in a tumorous ROI. Therefore, the total area of tumour ROI accepts less than 50% of tumour necrosis.

The reference ROI with the same size as the first, was placed contralaterally in a way that the brain tissues are similar and normal-appearing. A last and third ROI was positioned to obtain an arterial reference. This allows to know if a feeding artery is in the tumour, which can modify the patient's diagnosis. Knowing that CBV results are relative, the ratio of cerebral blood

volume correcting the leakage of gadolinium-based contrast agent effect caused by the blood-brain barrier breakdown was calculated as follows:

$$rCBV\ ratio = \frac{rCBV_{tumour}}{rCBV_{contralateral}}$$

4.7 Inter-software reproducibility

The two software packages studied, Intellispace and Olea, are both used in tumour evaluation at HUG. It depends on the radiologist who performs the post-processing. It is therefore important to know if the two programs provide the same result with the same diagnosis for the patient.

In order to compare the inter-software reproducibility, it is necessary that the methods used by software are identical (leakage correction for both). Therefore, each technique of both software products have been described to better compare them.

4.7.1 Leakage correction

In first place, among the methods proposed by Intellispace, only two adjust the leakage contrast effect: gamma variate and leakage correction. However, knowing that with a cerebral tumour, the vascular permeability is high, it is necessary to correct these effects during a tumour assessment. Therefore, manual and automatic AIF methods will not be compared in this study.

Secondly, knowing that gamma variate is an older method and is not a faithful representation of reality because of the fit to a gamma function, only the rCBV corrected by the leakage correction will be compared to the corrected values of Olea. Additionally, as previously written, these two techniques use the same reference for the leakage correction algorithm, from Boxerman and Weisskoff (Boxerman et al., 2006).

4.7.2 Adjacent tissue influence

During the various analyses, the ROI had to be corrected. Indeed, it was necessary to exclude from the regions of interest, the adjacent structures; either structures with high vascularity or necrosis. A subgroup was therefore created for the analysis to distinguish the subjects most at risk from being affected by the partial volume effect. It contains 17 DSC from 15 patients. They were selected according to the presence of vascularized structure or necrosis close to the tumour reference at ROI. Identifying them may unveil another vision.

4.7.3 Size ROI influence

A second subgroup was created based on the size of the ROI. In fact, small ROI's are strongly dependent on the partial volume effect. After analysis of the data, an empirical limit of 250mm^2 was decided. This subgroup contains 20 DSC from 16 patients. They were selected according to the size of tumour ROI, generally equivalent to contralateral.

4.7.4 Tumour influence

After excluding the variability due to the structures close to the regions of interest and their size, we still must explore the tumour variability. For this, a last subgroup was created containing 8 DSC from 6 patients. For these post-processing, ROI were placed differently from the rest of the study. Healthy structures for both ROI were chosen. The first included putamen and pallidum, while the second ROI was in a healthy frontal region.

4.8 Inter-operator reproducibility on Olea

Reproducibility between the two software is not the only profitable comparison to achieve in this context. As a matter of fact, at the HUG being a university hospital, several residents doctors perform the post-processing. Even though the regions of interest are controlled by a clinical professor, some human variability remains.

The second operator had a limited time and did the post-processing solely on Olea.

4.9 Intra-software reproducibility on Intellispace

Gamma variate was a method approved in the literature and still used clinically in many institutions. Since the arrival of new leakage correction algorithms, a question arises: is the difference between the two methods significant? This would allow to know if the diagnosis made before, with the gamma variate, still corresponds to the later diagnosis if it was made now with the leakage correction on Intellispace.

4.10 Statistical methods

All the data collected was processed with Stata/IC software (College Station, Texas, USA) version 15.0. For all tests, we assumed a statistically significant threshold of P=0.001.

In order to compare the software, the operators and the methods, an appropriate calculation is the intra-class correlation coefficient (ICC). This coefficient, adapted for continuous quantitative data, makes it possible to measure the degree of absolute agreement between two measurements. The sample range is sufficiently variable for this coefficient to be appropriate. The ICC for the inter-software and intra-software has been generated for the software and methods used in this study. While the ICC inter-operator has been calculated in such a way that the operator can be generalized to all the others. The recommended lower limit (Lee, Koh, & Ong, 1989) used in this study is at least 0.75.

In this situation, it is also possible to compute a Cohen's Kappa for categorical data. Indeed, as seen above, the literature concerning the interpretation of the rCBV ratio in gliomas is not unanimous. Some recommend a limit of 1.5–2, while others recommend 1.75. At HUG, the cut-off used is 1.5–1.7. Therefore, the results in this study were classified into three categories: no angiogenesis (<1.5), angiogenesis suspicion (1.5–1.7) and significant angiogenesis (>1.7). It allows to know if the clinical decisions between the various software, operators and methods corroborate. The recommended lower limit (Landis & Koch, 1977) used in this study is at least 0.6.

Scatter plots have also been created, although it is not the correlation or prediction that is under study. This allows to visualize the strength of the linear relation, as well as the dispersion of the data. It is also recommended in an agreement analysis (Bland & Altman, 1986).

The last graph, the Bland Altman is the most significative of the difference between two software, operators or methods. Created in 1983 by Douglas G. Altman and Martin Bland, it allows to evaluate the bias on the difference's average with the standard deviations (Altman & Bland, 1983). Adding to this graph the linear regression of the differences makes it possible to detect a proportional difference.

5. Results

5.1 Inter-software reproducibility

5.1.1 rCBV reproducibility between Intellispace and Olea

The reproducibility of rCBV between Intellispace and Olea is the most important of all the comparisons made in this study. As a matter of fact, it allows to know if the results and thus the diagnosis are identical with these two software products.

The relationship between Olea and Intellispace is represented in fig. 4. Data can be modelized by a linear regression (blue line). Its coefficient 0.72 is far from 1. Indeed, this means that when Olea obtains a rCBV ratio of 1, Intellispace obtains a rCBV ratio of only 0.72. The determination coefficient R^2, although significant (P<0.001), is as low as 54%, which shows a mean dispersion around the linear regression line that increases with the rCBV ratio. The identity line has been added (red line). It represents the slope if Olea was to provide exactly the same results as the Intellispace's leakage correction.

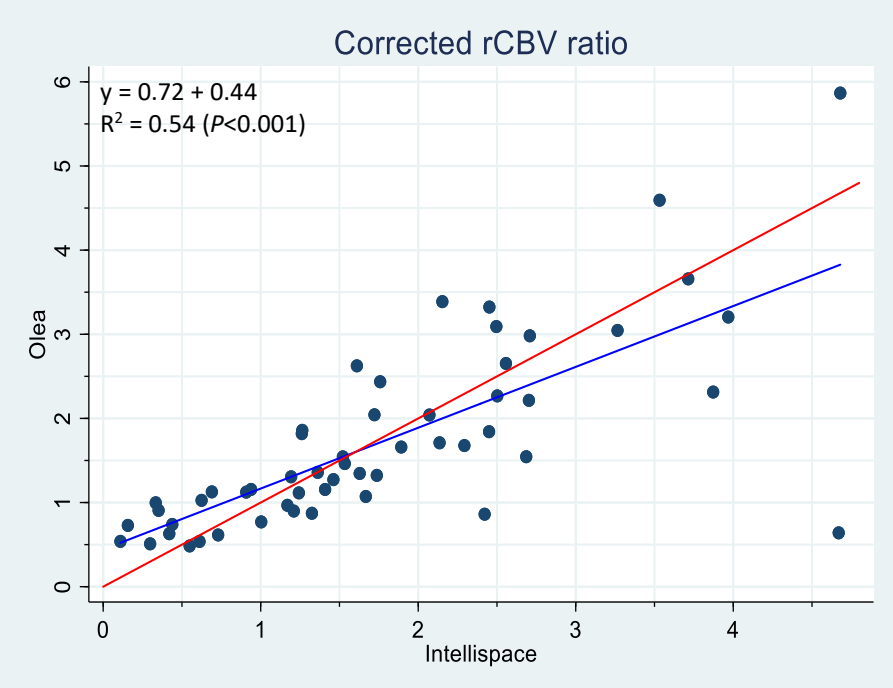

Figure 4: Scatter plot inter-software between Intellispace and Olea. The red line is the identity line, while the blue one is the data's linear regression line with its mathematical function and dispersion.

The Bland Altman graph (fig. 5), the most significative of the difference between two entities, has been represented with the upper and lower 95% limits of agreement. The mean, negative, but close to 0, shows a slight difference bias. In fact, the results obtained with Olea are systematically lower than those generated by Intellispace. The high standard deviation of 0.81 proves that when Olea gets a rCBV ratio of 1, Intellispace gets a ratio of 1.81. With a cut-off at 1.7, both software do not agree.

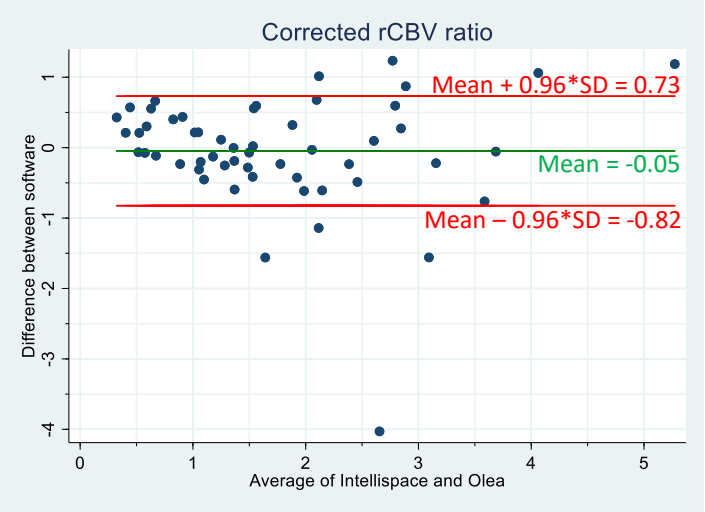

Figure 5: Bland Altman inter-software between Intellispace and Olea. The green line is the mean difference, while the red ones are the 95% limits of agreement.

The calculation of the intra-class correlation coefficient is significant (*P*<0.001) and moderate with 0.74. The ICC is just under the recommended limit which is 0.75. This means that the inter-software reproducibility is limited.

For categorical data, a table was generated to visualize the differences between clinical decisions (table 1). Twelve exams out of 54 do not have the same diagnosis according to the software used. Cohen's Kappa also has a significant (*P*<0.001) coefficient with 0.61. It just reaches the recommended limit of minimum 0.6.

		Intellispace			**Total Olea**
		No angiogenesis	Angiogenesis suspicion	Significant angiogenesis	
Olea	No angiogenesis	23	3	3	29
	Angiogenesis suspicion	0	1	3	4
	Significant angiogenesis	2	1	18	21
	Total Intellispace	25	5	24	54

Table 1: Angiogenesis diagnostic Intellispace versus Olea

Overall, the results between Olea and Intellispace are not similar. They are not discordant but reveal a concrete difference. Therefore, three specifics subgroups were created to try to explain this difference. All the statistical results obtained are presented in a summary table in order to compare them (table 8).

5.1.2 Adjacent tissue influence

The first subgroup was chosen to analyse the influence of adjacent tissues on regions of interest. To plot the data, a scatter plot has been computed (fig. 6). The green dots are those with necrosis or vascular structures near the ROI, while the blue dots are without. The green linear regression is the closest to the line of identity (red line). The outliers are mainly part of the green group.

The intra-class correlation coefficient is significant (*P*=0.001) and still moderate with 0.74. Nevertheless, Cohen's Kappa decreased with 0.47 and is non-significant (*P*=0.006). However, the small sample size of the group without necrosis or vascular structures near the ROI, must be considered. These results demonstrate that excluding patients affected by tissues adjacent to ROI does not significantly improve inter-software outcomes.

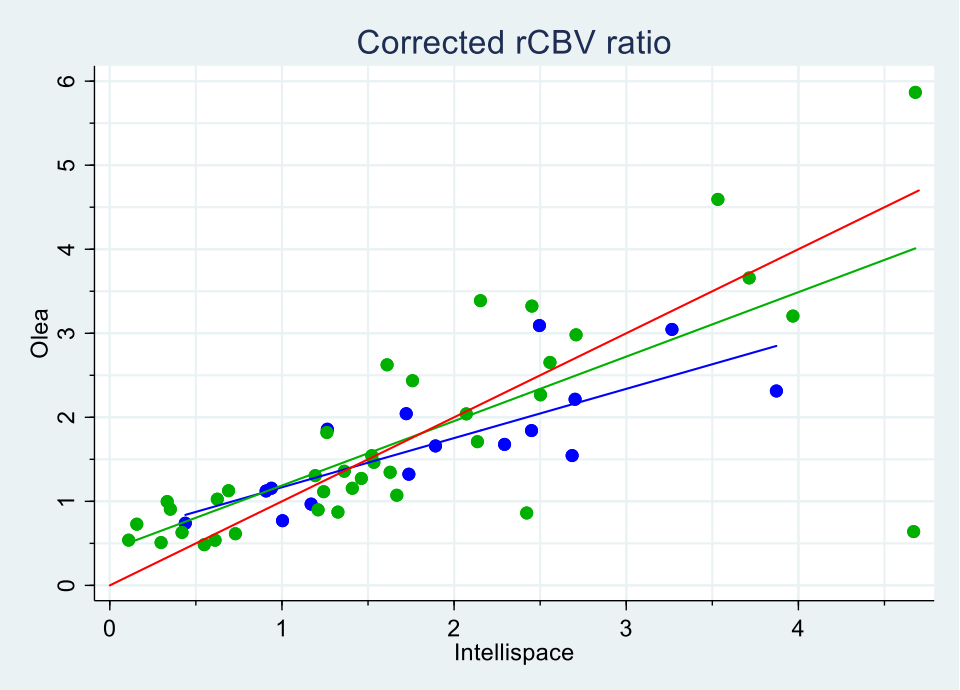

Figure 6: Scatter plot between Intellispace and Olea with the 1st subgroup. The greens dots are part of the group with necrosis and vascular structures near the ROI. While the blue dots come from the group without. The both groups are showed with them linear regression line. The red line is the identity line.

5.1.3 Size ROI influence

Inter-software variability may also be explained by the size of the tumour ROI. Both groups were represented in a scatter plot (fig. 7). The blue dots are those with the ROI area higher than 250mm^2. Their prediction line is close to the line of identity (red line) with a slope of 0.69 compared to the group with a small ROI (<250mm^2). The dispersion around this line is also better with a coefficient of determination of 0.71. While the coefficient of the group with small ROI is 0.40.

The intra-class correlation coefficient and Cohen's Kappa are significant (P<0.001) and better for the group with a large ROI rather than the total sample with 0.85 and 0.65 respectively. This means that the agreement between the two programs is good and that the consequent clinical decision may agree satisfactorily.

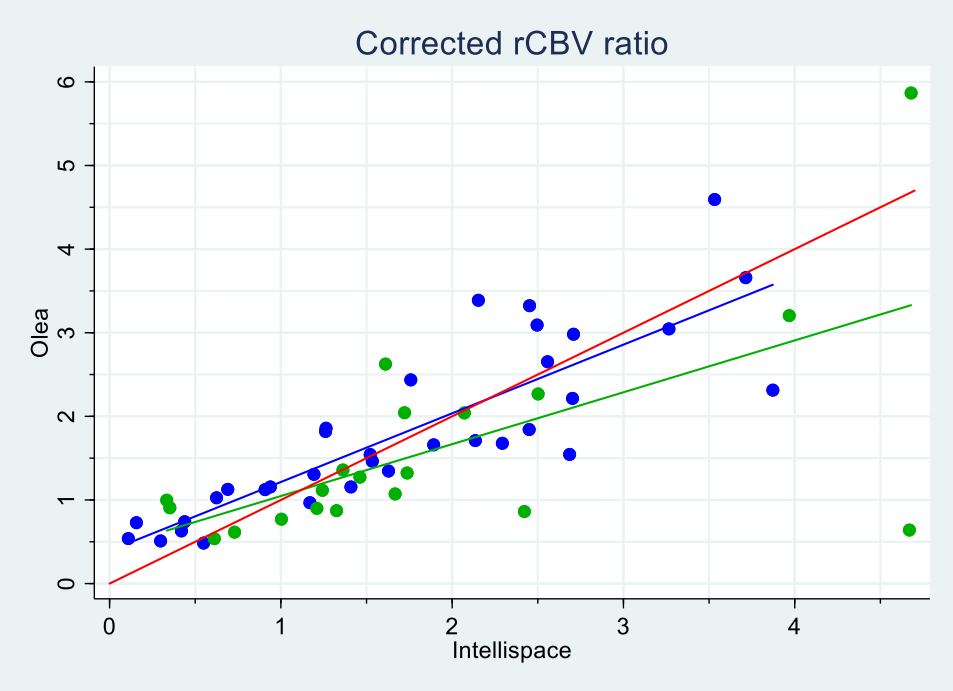

Figure 7: Scatter plot between Intellispace and Olea with the 2nd subgroup. The greens dots are part of the group with the ROI area lower than 250mm^2. While the blue dots come from the group with a ROI's area above 250mm^2. The both groups are showed with them linear regression line. The red line is the identity line.

5.1.4 rCBV's healthy structure

At this step of the study, tumour results differ between Intellispace and Olea. Therefore, a third analysis was performed to determine if this difference is caused by tumour variability. The last subgroup created allows to know if healthy structures have the same rCBV result between the two software. Knowing that cerebral blood volume is relative, it was necessary to create healthy structural ratios. In the scatter plot (fig. 8), it is possible to notice that despite an outlier, the data agree well and are scattered around the identity line. The table of data confirms this (table 2). The calculation of the ICC is not adapted in this case because the sample size is too small.

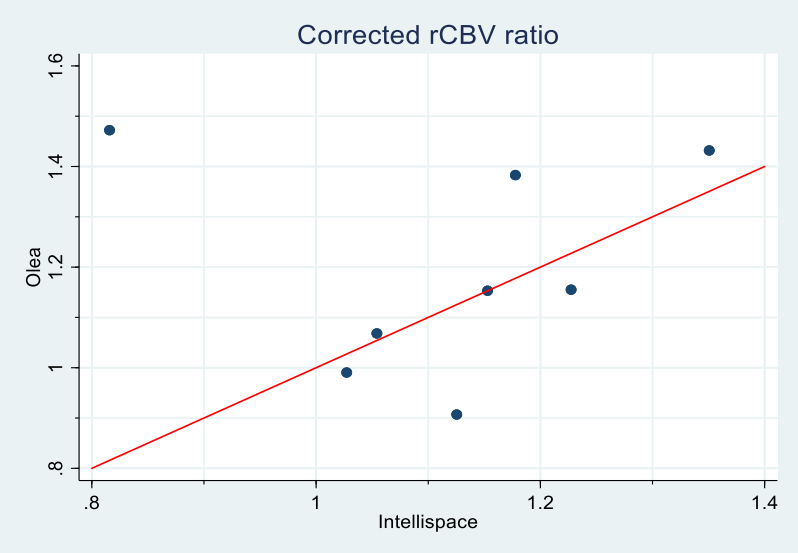

Figure 8: Scatter plot between Intellispace and Olea with the 3rd subgroup. Correlation between rCBV ratio from healthy structures are showed. The identity line is represented in red.

Intellispace			Difference	Olea		
ROI 1	ROI 2	**Ratio rCBV**		**Ratio rCBV**	ROI 1	ROI 2
66.87	81.97	**0.82**	0.65	**1.47**	1.59	1.08
83.55	74.24	**1.13**	0.22	**0.91**	1.56	1.72
233.65	190.36	**1.23**	0.07	**1.16**	2.68	2.32
150.35	111.32	**1.35**	0.08	**1.43**	3.68	2.57
221.47	188.05	**1.18**	0.20	**1.38**	2.60	1.88
236.50	230.22	**1.03**	0.04	**0.99**	2.08	2.10
435.41	377.66	**1.15**	0.00	**1.15**	2.41	2.09
376.79	357.42	**1.05**	0.02	**1.07**	3.29	3.08

Table 2: Difference within the 3rd subgroup between Intellispace and Olea. The first ROI are drawn around the putamen and the pallidum, while the second ROI was contouring a healthy frontal region. The rCBV ratios are calculated and the difference between Intellispace and Olea are shown. The smallest difference is in green whereas the highest is in red.

5.1.5 Visual assessment of rCBV

During a tumour evaluation, it is necessary to always assess the semi-quantitative results, but also visually the generated map. Therefore, some cases will be compared visually between the two programs.

The rCBV results are not of the same range between the two software, which is noticeable with image's colorscale (fig. 9 and 10). Value for data from Intellispace is 100x greater than Olea's. Consequently, considering this factor, the colorscales have been adapted to each other. Yet it is still possible to see visually a difference between the two maps produced and the regions of interest. Indeed, with patient n°88 (fig. 9), the contralateral reference ROI (ROI n°2) is a little bit anterior on Olea than on Intellispace. However, the same operator did the post-processing on both software. Regarding the patient's rCBV ratio (table 3), the difference between the two programs is insignificant.

Corrected rCBV	ROI tumour	ROI contralateral	**Ratio rCBV**
Intellispace	600.50	161.68	**3.71**
Olea	7.51	2.03	**3.70**

Table 3: rCBV of patient n°88 between Intellispace and Olea

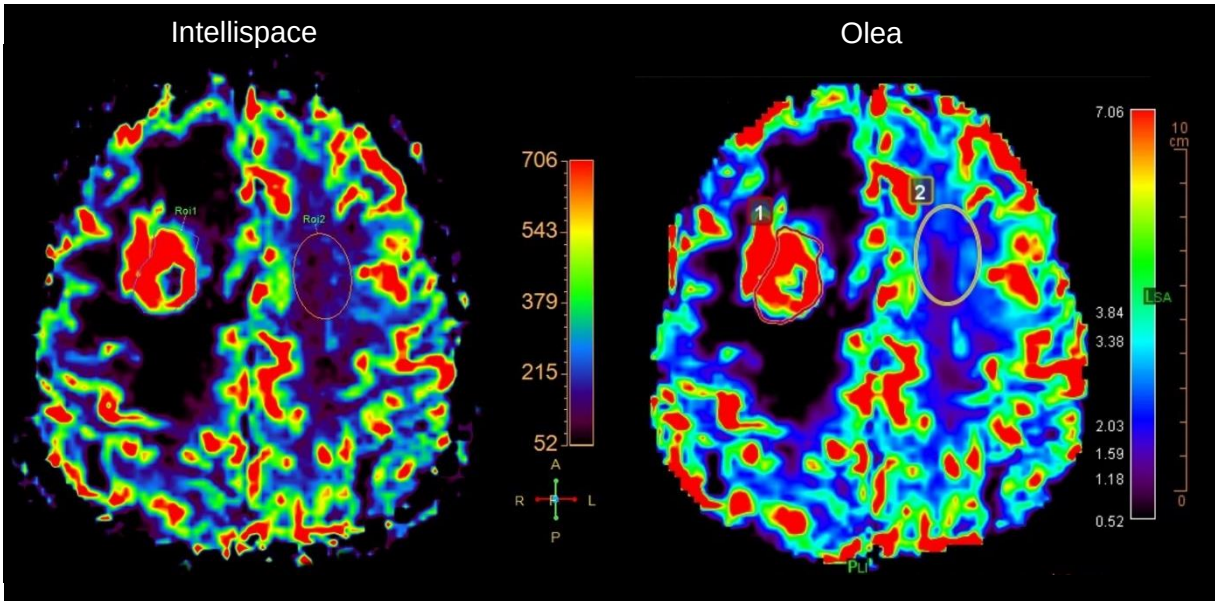

Figure 9: Patient n°88 on Intellispace and Olea

The second patient presented (n°41, fig. 10) confirms the presence of intra-operator variability. In fact, the ROI of reference is slightly more externally on Olea than on Intellispace. Regarding his rCBV ratio (table 4), there is a big difference between the two software, a spread of 1.19. This difference can be explained because of the size of the ROI, less than 150mm^2 with a percentage of partial volume effect higher than the first example. However, since both ratios are greater than 1.7, the clinical decision would be the same.

Corrected rCBV	ROI tumour	ROI contralateral	**Ratio rCBV**
Intellispace	643.50	137.51	**4.68**
Olea	7.92	1.35	**5.87**

Table 4: rCBV of patient n°41 between Intellispace and Olea

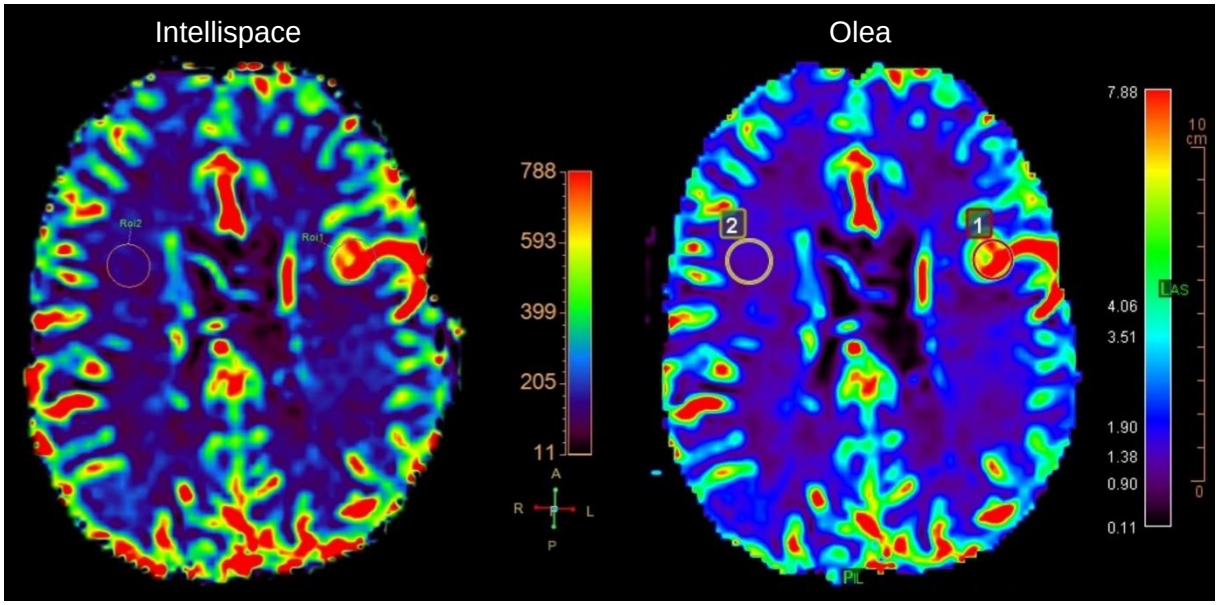

Figure 10: Patient n°41 on Intellispace and Olea

5.2 Inter-operator reproducibility on Olea

5.2.1 rCBV reproducibility between two operators

Reproducibility between two operators is essential in a clinical context. It allows to know if the results are identical between two trained users.

In the scatter plot (fig. 11), it is possible to visualize a small significant (*P*<0.001) dispersion of the measurements around the linear regression line which increase with the rCBV ratio with an adjustment coefficient of 80%. The regression coefficient is close to the identity line. This means that when an operator obtains a rCBV ratio of 1, the second operator gets 1.22.

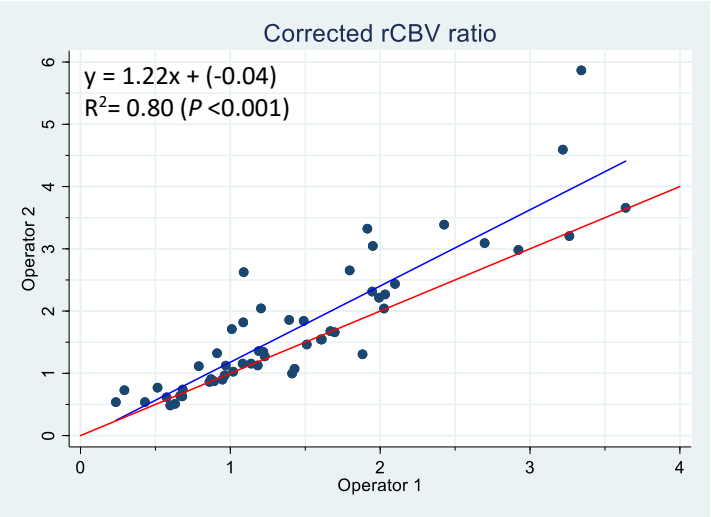

Figure 11: Scatter plot inter-operator between two trained users. The red line is the identity line, while the blue one is the data's linear regression line with its mathematical function and dispersion.

The mean differences obtained in the Bland Altman graph (fig. 12) demonstrates a slightly systematic bias between the two operators. Almost 80% of the measurements are between the upper and lower limits. The standard deviation is quite small with 0.54.

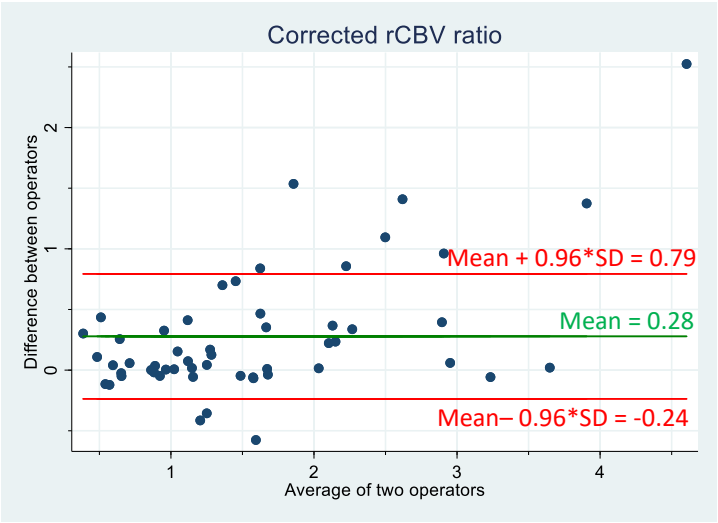

Figure 12: Bland Altman inter-operator between two trained users. The green line is the mean difference, while the red ones are the 95% limits of agreement.

The intra-class correlation coefficient is good, almost excellent and significant (*P*<0.001) with 0.81. This means that the results between the two operators have a good agreement. The inter-operator reproducibility is significantly similar.

Concerning the diagnosis, there is a little variability. Indeed, Cohen's Kappa is satisfactory and significant (*P*<0.001) with 0.73. Operators agree on clinical decision after post-processing.

5.2.2 Visual assessment of rCBV

For the visual assessment of inter-operator reproducibility, two representative cases have been selected.

In first place, patient n°11 (fig. 13) is a good example of the difference when generating maps between two operators. Indeed, although the colorscales are identical between the two images, there are visible differences in the contrast obtained. In the frontal and occipital region, relative cerebral blood volume is increased with the second operator. However, in the tumour ROI, the rCBV is higher with the 1st operator. After analysing the rCBV ratio (table 5), there is a difference between the two operators. Knowing that the cut-off is at 1.7, the diagnosis of the patient may not be the same according to the radiologist who performs the post-processing.

Corrected rCBV	ROI tumour	ROI contralateral	**Ratio rCBV**
1st operator	5.11	2.75	**1.86**
2nd operator	4.01	2.88	**1.39**

Table 5: rCBV of patient n°11 between the two operators

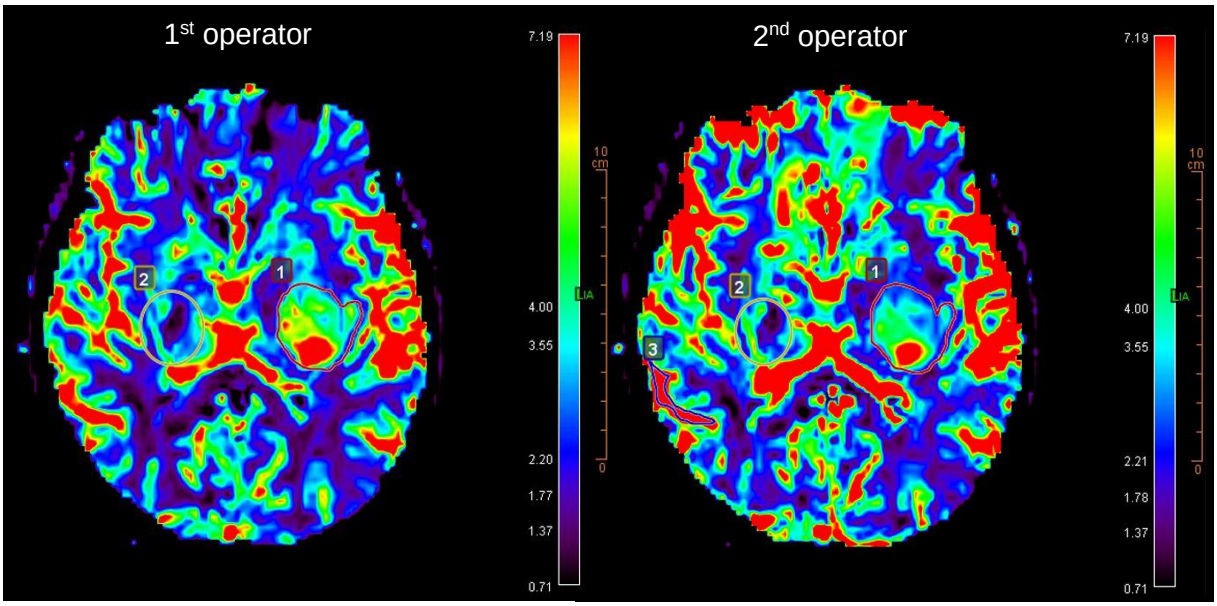

Figure 13: Patient n°11 with the two operators

Secondly, these images coming from the patient n°39 (fig. 14) confirms the difference when generating the maps and allows demonstrating human variability despite a common training and correction. The contours drawn around the region of tumour interest are slightly different between the two operators, as well as the contralateral ROI. Indeed, the second ROI is not in the same orientation, which modifies the results obtained from the rCBV. There is a real difference in the rCBV ratio between the two operators (table 6) which is equal to 0.51. However, knowing that the decisional cut-off is at 1.7, in both situations, the clinical follow-up might be the same.

Corrected rCBV	ROI tumour	ROI contralateral	**Ratio rCBV**
1st operator	5.65	1.70	**3.32**
2nd operator	5.59	2.92	**1.91**

Table 6: rCBV of patient n°39 between the two operators

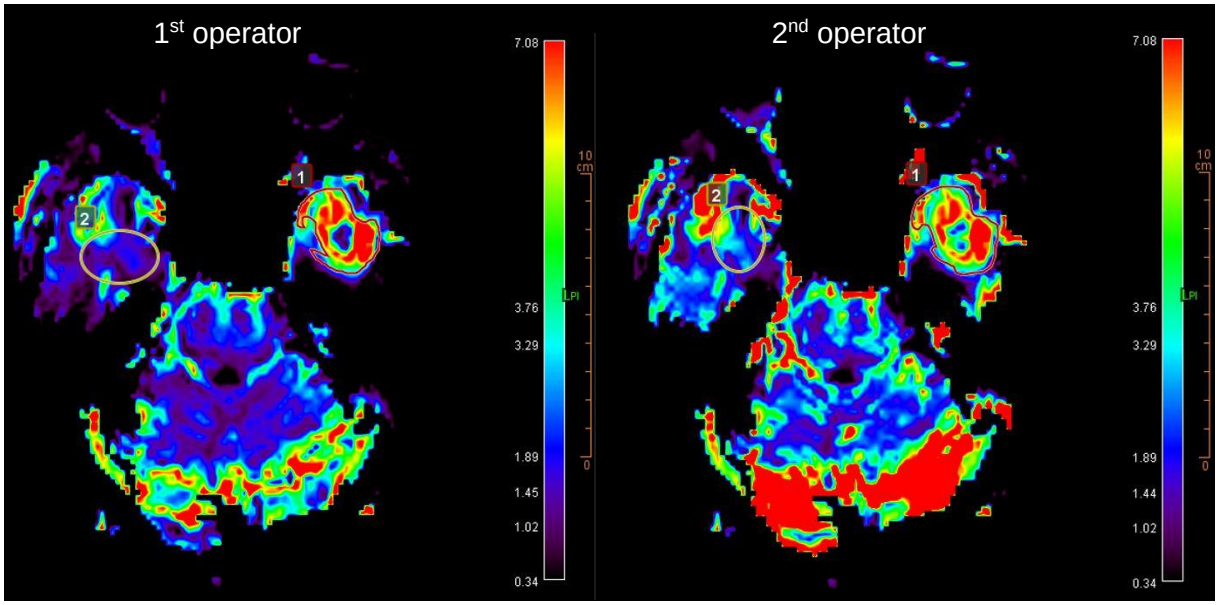

Figure 14: Patient n°39 with the two operators

5.3 Intra-software reproducibility on Intellispace

5.3.1 rCBV reproducibility between leakage correction and gamma variate

The reproducibility between leakage correction and gamma variate within Intellispace is the last evaluation in this study. This will help to know if the diagnosis is the same between these both methods.

To begin with this comparison, two examinations had to be removed from the sample because gamma variate did not provide results in the tumorous ROI. One of the two cases will be studied in the visual assessment of rCBV.

For the rest of the sample, the determination coefficient of the scatter plot (fig. 15) is significant (P<0.001) and good at 80%. There is little dispersion of measurements around the linear regression line. Its coefficient is close to 1, with 0.83. This means that the results obtained between these two methods are almost identical.

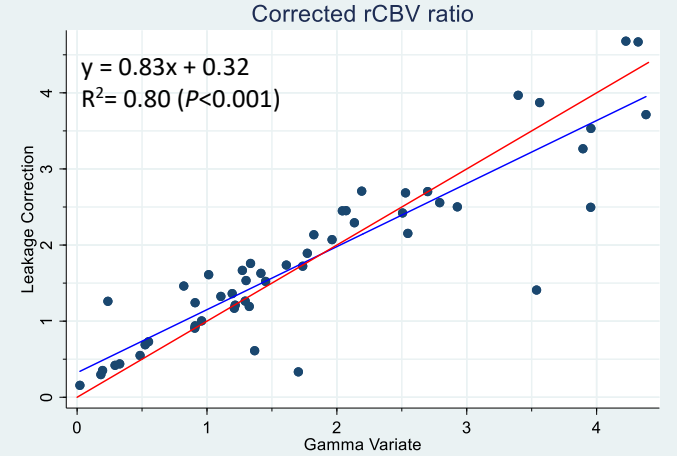

Figure 15: Scatter plot intra-software on Intellispace between leakage correction and gamma variate. The red line is the identity line, while the blue one is the data's linear regression line with its mathematical function and dispersion.

The Bland Altman (fig. 16) shows a very slight bias and therefore not significant. The mean difference is really close to 0. There are really few differences in the results obtained between leakage correction and gamma variate.

The intra-class correlation coefficient is significant (P<0.001) and excellent with 0.90. This means that there is an excellent agreement between the two methods used.

Concerning the diagnosis, there is a good reproducibility. Indeed, Cohen's Kappa result's is satisfactory and significant

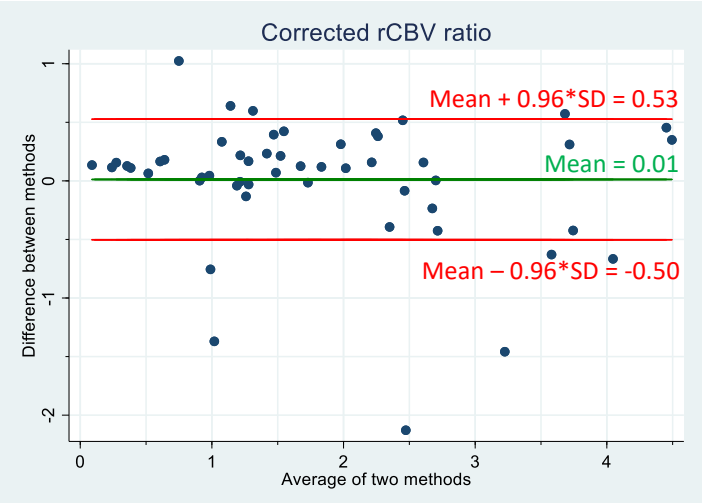

Figure 16: Bland Altman intra-software on Intellispace between leakage correction and gamma variate. The green line is the mean difference, while the red ones are the 95% limits of agreement.

(*P*<0.001) with 0.69. Methods from Intellispace agree on clinical's decision-taking after post-processing.

5.3.2 Visual assessment of rCBV

For the visual comparison, on the patient n°63 (fig. 17) it allows to point-out that with the same colorscale on both methods, the data will be different. In general, the values are lower with the leakage correction. With the gamma variate, in tumour ROI, there is more colour variation. Yet by analysing the ratio rCBV (table 7), the difference is small and the diagnosis would be the same.

Corrected rCBV	ROI tumour	ROI contralateral	**Ratio rCBV**
Leakage correction	130.69	52.36	**2.50**
Gamma variate	203.33	73.90	**2.75**

Table 7: rCBV of patient n°63 between leakage correction and gamma variate from Intellispace

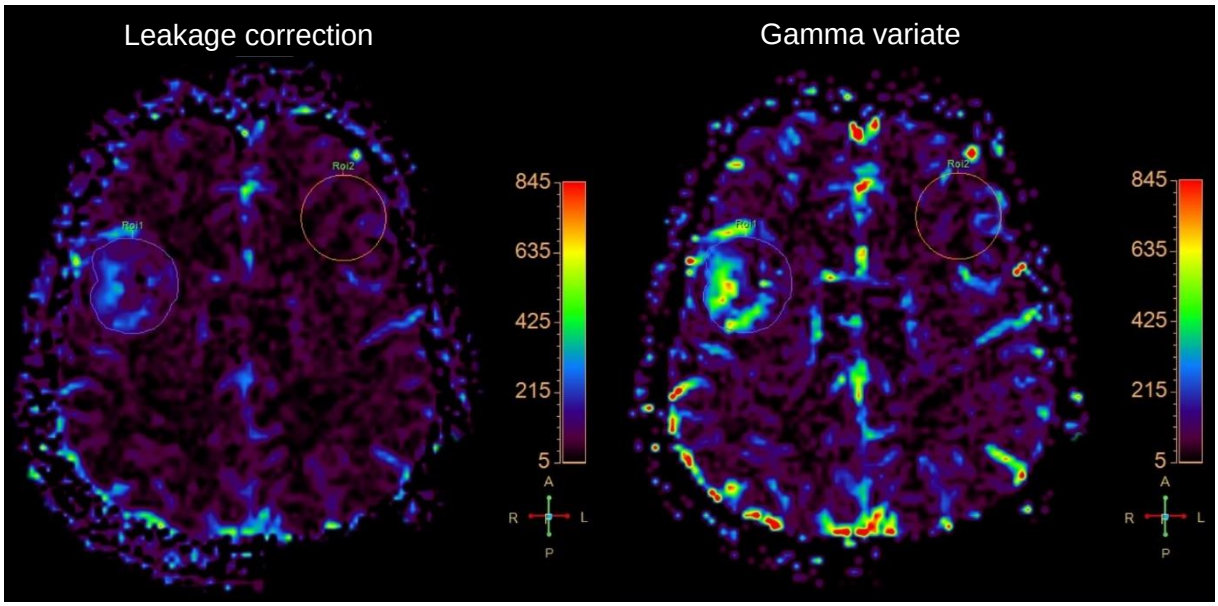

Figure 17: Patient n°63 with leakage correction and gamma variate

The second example (fig. 18) is one of the patients with no rCBV results with gamma variate. The tumour lesion, before being resected by craniotomy, was in the right temporopolar region. Thanks to the morphologic T1- and T2-weighted sequences; it is possible to notice that the cavity is filled with cerebrospinal liquid which is therefore not vascularized. Because of the proximity of the cavity, the tumour ROI may be affected by the partial volume effect. This may explain the inability of gamma variate to generate a result in this region. In addition, the size of the ROI is small with a total area of only 220.50 mm^2.

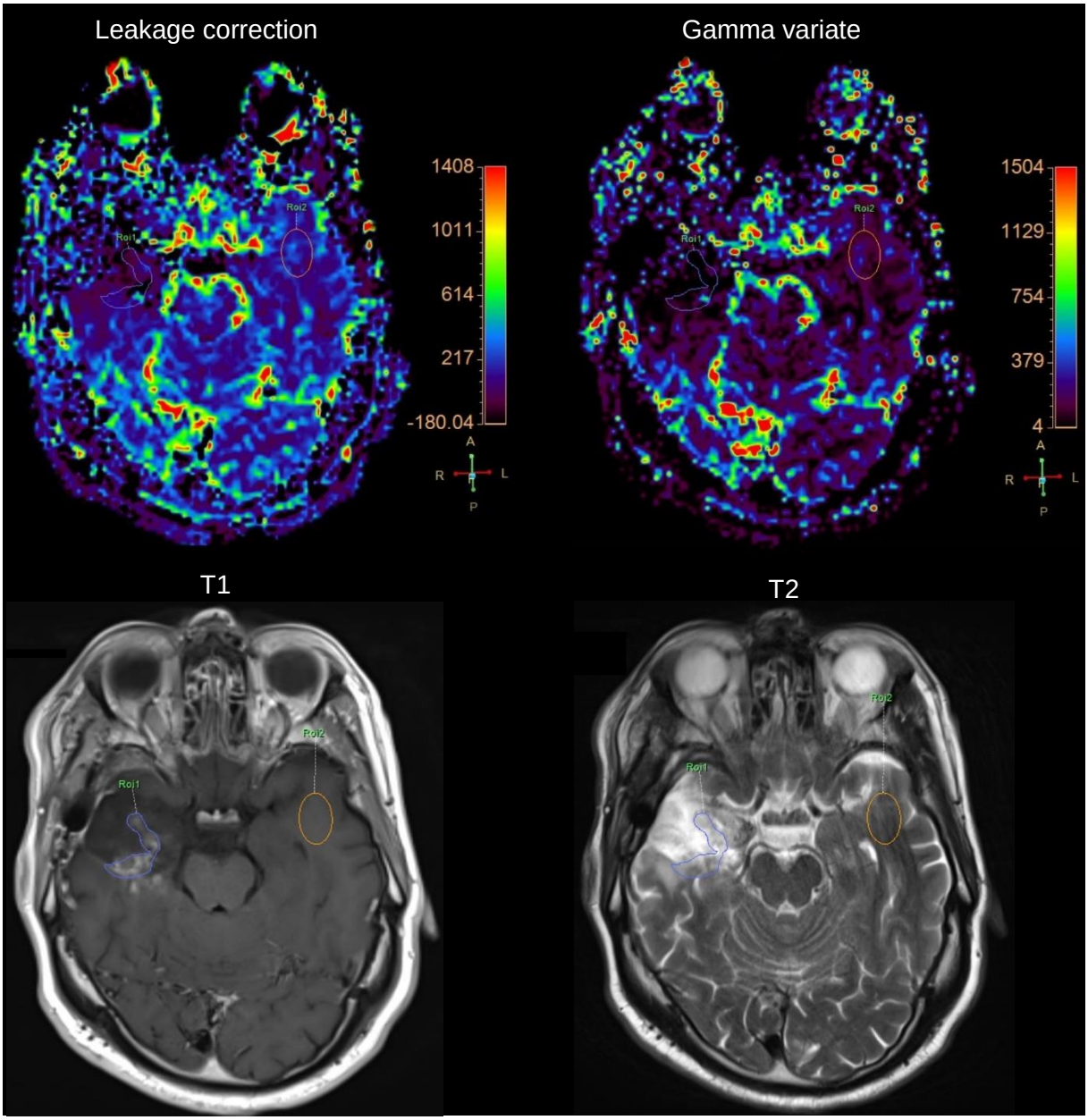

Figure 18: Patient n°33 with leakage correction, gamma variate and morphologic T1- and T2-weighted imaging

5.4 Summary table of results

In order to be able to evaluate the various reproducibilities overall, a summary table of all the statistical results has been designed.

Reproducibility	Scatter plot		Bland Altman		Intra-class correlation coefficient (>0.75)	Cohen's Kappa (>0.6)
	y = ax + b	R^2	Mean	SD		
Inter-software	a= 0.72*	0.54*	-0.05	0.81	0.74*	**0.61***
Healthy adjacent tissue					*0.74**	*0.47*
Large ROI's size					***0.85****	***0.65****
Inter-operator	a= 1.22*	0.80*	0.28	0.54	**0.81***	**0.73***
Intra-software	a= 0.83*	0.80*	0.01	0.54	**0.90***	**0.69***

Table 8: Summary table of study's results with the three mains reproducibilities. The subgroups are represented in italics. In bold are showed the results above the lower limit recommended.

*highly significant ($P \leq 0.001$)

6. Discussion

6.1 Inter-software reproducibility

The main purpose of this study is the inter-software reproducibility between Intellispace and Olea. These two programs are used daily in many hospitals, so it is important that the results obtained correspond.

The scatter plot has demonstrated that the data prediction line is far from the line of identity. Moreover, the coefficient of determination is low with 54%, which proves a mean dispersion of the data. In the Bland Altman, the mean difference is very close to 0 with -0.05. However, the standard deviation is the largest of all reproducibilities at 0.81, compared with 0.54 for the other two (table 8). The coefficient obtained for the intra-class correlation is just below the recommended limit with 0.74, instead of 0.75. While Cohen's Kappa just reaches the recommended lower limit of 0.60.

Following the analysis of the results, it is possible to notice that there is a non-negligible difference in the ratio rCBV obtained for each software. In addition, although Cohen's Kappa

barely reaches the recommended limit, twelve out of 54 exams do not agree on the diagnosis, which is not acceptable in a clinical context. This discrepancy is underlined with the highest standard deviation of the study. Indeed, the high standard deviation of 0.81 proves that when Olea gets a rCBV ratio of 1, Intellispace can get a ratio of 1.81 which is not good because the cut-off is at 1.7, the therapeutic follow-up of the patient would not be the same.

To explain this difference in the rCBV ratio between the two software products, three hypotheses were emitted. In first place, this can be caused by the partial volume effect. Indeed, the adjacent structures inclusion within the ROI can alter the calculation of the rCBV. Secondly, this negative effect can also be underlined thanks to the small ROI, because they are more affected by the partial volume effect. At last, after eliminating this variability in cases with high-grade gliomas, it remains only to exclude the pathological factor. In evaluating healthy regions, the last variability involved come from respective mathematical models and how software makers code it.

Contouring regions of interest, excluding necrosis and proximate vascular structures, reduces the partial volume effect caused by adjacent tissues. However, according to the statistical analysis, the results are still showing important differences in clinical reality and do not improve inter-software reproducibility.

Nevertheless, drawing large ROI with a total area of at least 250mm^2 provides acceptable inter-software reproducibility. Indeed, large ROI are less affected by the partial volume effect because the percentage of the region affected is low relative to the total area.

After excluding the partial volume effect using the first two subgroups, the last subgroup created compared the rCBV of healthy regions. The correlation between healthy regions is quite good, apart from a visible outlier in fig. 9. In general, the results are relatively equivalent to each other, except one that has a difference of 0.65 in table 2, which is high and not good for a clinical context.

6.2 Inter-operator reproducibility on Olea

Inter-operator reproducibility is very important in a clinical context. The statistical results show that there is a good agreement between the results on Olea. Indeed, the dispersion of the data in the scatter plot is small with an R^2 at 0.80. The mean difference on the Bland Altman is close to 0. This means that there is little difference between the rCBV ratios obtained for each

operator. However, this difference increases with the rCBV ratio. The intra-class correlation coefficient and Cohen's Kappa are good with 0.81 and 0.73 respectively, above the recommended limits.

This small variation in the results is clinically acceptable. Furthermore, the operators agree on the diagnosis of the patient. These results demonstrate that Olea is robust with several operators.

6.3 Intra-software reproducibility on Intellispace

Regarding the last analyse of this study, the statistical results show an excellent agreement between the leakage correction and gamma variate on Intellispace with an intra-class correlation coefficient at 0.90. Dispersion is one of the smallest of all comparisons in this study; mean difference is the closest to 0 and clinical judgment from DSC post-processing is consistent. The results are totally acceptable for a clinical reality.

However, in two out of 54 cases, leakage correction gets a quantitative result, while gamma variate does not. This can be explained by the proximity of the ROI to non-vascularized structures, but also by its small size (<250mm^2). These two situations prove that leakage correction of Intellispace with the Boxerman-Weisskoff model is more robust than gamma variate.

6.4 Limitations

6.4.1 Intra-operator variability

Despite the rigor used, each human is affected by a variability of its own. The shape, position and orientation of each ROI have been checked numerous times to be as similar as possible between the two programs. Nevertheless, differences between the ROI created by the same operator exist. It is impossible to generate a compatible region of interest file between the two software, so it is necessary to draw it each time. This limit only affects the inter-software reproducibility, because in the intra-software reproducibility; the ROI are the same.

6.4.2 Sample size

After having analysed the variability of the scope, even if it is non-exhaustive, the statistical conditions will be assessed.

To begin, the Bland Altman graph could have contained more patients in order to have a more relevant interpretation. Martin Bland himself recommends a sample of at least 100 subjects, even 200 patients (Bland, 2004). It was not possible to obtain the entire sample, but this limit does not prevent us from reaching appropriate conclusions.

Furthermore, one of the subgroups used in inter-software reproducibility has a small sample size. Indeed, the subgroup with necrosis or vascularized structure near the ROI is very large, so not many subjects are without this partial volume effect.

6.5 Perspectives

Therefore, the evaluation of the influence of the presence of necrosis or vascularized structure near the ROI on relative cerebral blood volume could be the subject of a future study. In fact, a more adequate sample size could allow to know if this influence is one of the causes of the inter-software's poor reproducibility.

A larger sample size can also be used to complete the comparison of ROI drawn in a healthy region. With a sufficient sample, it is possible to carry out the statistical tests which allow to demonstrate a difference between the model of each software and its implementation.

To confirm this difference between Intellispace and Olea, performing this comparison with an MRI phantom simulating flow eliminates the human variability created by the patient. It is thus necessary to transfer the images acquired in the two post-processing software, which can lead to a slight distortion of the data. To avoid this, it is possible to create a well-defined dataset insertable directly into the software. By considering all the limitations, a difference between the model of each software can be demonstrated.

Regarding the inter-operator comparison, it might have been interesting to add more operators in order to obtain more accurate statistical results. This can confirm Olea's robustness against different operators.

7. Conclusions and recommendation

Post-processing algorithms correcting for the leakage of gadolinium-based contrast agent effect caused by the blood-brain barrier breakdown for a DSC-MRI are recommended. However, it is important to evaluate the reproducibility of the methods and software in order to be able to compare the results between the different studies and clinical institutions.

7.1 Inter-software reproducibility

The variability between rCBV ratios from Intellispace and Olea is not ideal in a clinical setting. Despite this difference, the clinical opinion resulting from the post-processing of the DSC was identical between the two programs, which is important. This means that institutions would perform the same follow-up regardless of the software used.

- To improve the variability between them, it is necessary to draw a large ROI with a total area of at least 250mm^2.
- This alleviates the partial volume effect which is the first cause of this difference. However, being careful to eliminate vascular structures and ROI necrosis does not improve this variability.
- The second reason that explains this difference between the two programs is the model used by each. Although they both use the Boxerman-Weisskoff model, in one out of 8 cases (12.5%), the rCBV ratio of healthy structures is different for no apparent reason (position, size and orientation of the two ROI, tissue composition, proximity of a vessel, etc.), which is not optimal.

7.2 Inter-operator reproducibility on Olea

The variability of the rCBV ratio between several operators on Olea is satisfactory, although there are differences in the positioning of the ROI. This means that in the same institution, all trained operators perform the post-processing in their own way. However, they get the same results and a similar clinical decision and therefore between many institutions using Olea Sphere v.3.0 - SP6.

7.3 Intra-software reproducibility on Intellispace

The variability of the rCBV ratio between gamma variate and the Boxerman-Weisskoff model on Intellispace is excellent. Although the fitting to a gamma variate function is no longer recommended, the clinical decision from DSC-MRI is similar.

To summarize, although software use the same models, there may be differences in how to code the Boxerman-Weisskoff algorithm. Indeed, each post-processing software has its own way of handling the model, which can affect the results.

Conflict of interest statement

No author has financial interest in the subject matter, the software or equipment connected with this research.

Summary in french – Résumé en français

Introduction

L'imagerie de perfusion T2* par résonance magnétique est une des techniques les plus utilisées dans la clinique pour quantifier la perfusion cérébrale et la néoangiogénèse à l'aide du premier passage d'un bolus de gadolinium. Afin d'éliminer l'effet de fuite de l'agent de contraste causé par la rupture de la barrière hémato-encéphalique, il est recommandé d'utiliser un algorithme après l'examen. Pour cela, il existe des logiciels de post-traitement avec de modèles mathématiques tels que le gamma variate ou le modèle de Boxerman-Weisskoff.

Problématiques

Le but principal de cette étude est d'évaluer la concordance des résultats obtenus entre Intellispace Portal et Olea Sphere lors du post-traitement de la perfusion T2*. En effet, plusieurs logiciels sont disponibles sur le marché, donc il est important que l'avis clinique découlant de l'analyse de l'examen (néoangiogénèse significative ou non) soit semblable.

La deuxième question posée consiste à analyser la reproductibilité entre deux opérateurs sur Olea Sphere. Dans la clinique, il n'existe généralement pas une personne assignée à ce post-traitement, c'est pourquoi il est important que le logiciel fournisse toujours le même résultat.

La dernière problématique permet d'étudier la variabilité entre le gamma variate et le nouvel algorithme de Boxerman-Weisskoff sur Intellispace Portal. Cela permet de déterminer si l'avis clinique découlant du gamma variate correspond toujours à celui de Boxermann-Weisskoff.

Matériel et méthode

Le deuxième opérateur dans cette étude était le Dr Wanyanga, junior en oncologie à l'hôpital de Fribourg avec une année d'expérience. Nous avons tous les deux été formés par la Dre Vargas, senior en neuroradiologie avec 22 années d'expérience. La récolte de données a duré plusieurs mois durant l'année 2018, de mars à novembre.

L'échantillon de départ comprend 46 patients atteints d'un astrocytome ou d'un glioblastome avec 72 examens réalisés à l'aide d'une Imagerie par Résonance Magnétique de 3 Tesla. En fonction de la nature de la tumeur, sa localisation, ainsi que la qualité d'image, 18 perfusions cérébrales T2* ont été exclues. L'échantillon final de cette étude comprend donc 54 examens appartenant à 35 patients (rapport H/F : 2.19:1 ; âge moyen : 59 ans [min : 27, max : 73]). Des sous-groupes ont ensuite été créés à partir de cet échantillon pour l'analyse des résultats.

Les examens ont tous été analysés par deux logiciels capables de corriger l'effet de fuite d'un agent de contraste à base de gadolinium à l'aide du modèle de Boxerman-Weisskoff : Intellispace Portal version 9.0 et Olea Sphere version 3.0 – SP6, abrégés par Intellispace et Olea. Le post-traitement des perfusion T2* a permis d'obtenir le volume sanguin cérébral relatif (rCBV) normalisé avec une région controlatérale saine : le rapport rCBV.

Résultats

Dans l'ensemble, l'analyse du diagramme de dispersion, du Bland Altman, du coefficient de corrélation intra-classe (ICC) et du Cohen de Kappa pour la décision clinique, révèle une différence concrète entre Intellispace et Olea. En effet, cela démontre que le rapport rCBV obtenu n'est pas similaire entre les deux. C'est pourquoi, trois sous-groupes spécifiques ont été créés pour essayer d'expliquer cette différence inacceptable pour un contexte clinique.

Le premier sous-groupe a été choisi pour analyser l'influence des tissus adjacents sur les régions d'intérêt (ROI). Les cas ont été sélectionnés par rapport à la proximité de zone nécrosée ou de structures vascularisées du ROI tumoral qui peut produire un effet de volume partiel. L'analyse du diagramme de dispersion avec le sous-groupe, de l'ICC et du Cohen de Kappa démontre qu'exclure les patients dont le ROI est proche d'une nécrose ou d'une structure vascularisée n'améliore pas significativement les résultats inter-logiciels.

La variabilité inter-logicielle peut s'expliquer également grâce à la taille du ROI. Plus il est petit, plus il est affecté par l'effet de volume partiel. Le deuxième sous-groupe a été sélectionné en fonction de la taille de la région d'intérêt tumorale (±250mm^2). L'analyse avec outils statistiques a démontré une bonne reproductibilité inter-logicielle avec des grands ROI (>250mm^2).

À ce stade de l'étude, les résultats tumoraux diffèrent entre Intellispace et Olea. C'est pourquoi, une troisième analyse a été réalisée afin de définir si cette différence est due à la variabilité tumorale. Le dernier sous-groupe créé permet donc de savoir si des structures saines ont le même rapport rCBV entre les deux logiciels. D'après les résultats, malgré un cas, les données sont bien corrélées et peu dispersées autour de la ligne d'identité du diagramme de dispersion.

La variabilité inter-opérateur est essentielle dans le cadre d'un hôpital universitaire. Les outils statistiques (diagramme de dispersion, Bland Altman, ICC et Cohen de Kappa) démontrent une bonne reproductibilité entre plusieurs opérateurs.

La reproductibilité entre le modèle de Boxerman-Weisskoff et le gamma variate au sein d'Intellispace est la dernière évaluation de cette étude. Pour cette comparaison, deux examens

ont dû être retirés de l'échantillon, car le gamma variate n'a pas fourni de résultats au niveau du ROI tumoral. Pour le reste de l'échantillon, l'analyse statistique est excellente.

Discussion

Il ne faut pas oublier de prendre en compte les limitations. En effet, malgré la rigueur utilisée, il est impossible de créer un fichier du ROI compatible entre les deux logiciels, donc une variabilité intra-opérateur existe. De plus la taille d'échantillon est petite pour le Bland Altman ou pour les sous-groupes mais cela n'empêche pas d'obtenir des conclusions appropriées.

Conclusions et recommandation

La variabilité entre les rapports rCBV d'Intellispace et d'Olea n'est pas idéale dans un contexte clinique. Malgré cette différence, l'avis clinique découlant du post-traitement de la perfusion T2* se rejoint entre les deux logiciels, ce qui est important. Cela signifie que dans l'ensemble, les institutions réalisent le même traitement indépendamment du logiciel utilisé.

Pour améliorer la reproductibilité inter-logicielle, il est nécessaire de dessiner des grands ROI avec une aire totale d'au minimum 250mm^2. Cela permet d'atténuer l'effet du volume partiel qui est la première cause de cette différence. Cependant, faire attention à éliminer les structures vascularisées et la nécrose du ROI n'améliore pas cette variabilité. La deuxième raison qui explique la différence entre les deux logiciels est le modèle utilisé. Bien qu'ils utilisent tous les deux le modèle de Boxerman-Weisskoff, dans un cas sur 8 (12.5%), le rapport rCBV de structures saines est vraiment différent sans raison apparente (position, orientation et taille des ROI, composition du tissu, proximité d'un vaisseau, etc), ce qui n'est pas optimal.

La reproductibilité du rapport rCBV inter-opérateur sur Olea est satisfaisante. Des différences existent dans le positionnement du ROI. Cela signifie que dans une même institution, tous les opérateurs formés réalisent le post-traitement différemment. Cependant ils obtiennent des résultats similaires entre plusieurs institutions utilisant Olea Sphere v.3.0 - SP6.

La variabilité du rapport rCBV entre le gamma variate et le modèle mathématique de Boxerman-Weisskoff sur Intellispace est petite, ce qui est un excellent résultat. Cependant le nouvel algorithme est plus robuste, car il a pu générer un résultat pour tous les patients de l'échantillon, contrairement au gamma variate.

Pour résumer, bien que des logiciels utilisent le même modèle, il peut exister des différences dans la manière de coder l'algorithme de Boxerman-Weisskoff. En effet, chaque logiciel de post-traitement a sa propre manière de traiter le modèle, ce qui peut affecter les résultats.

References

Al-Okaili, R. N., Krejza, J., Wang, S., Woo, J. H., & Melhem, E. R. (2006). Advanced MR Imaging Techniques in the Diagnosis of Intraaxial Brain Tumors in Adults. *RadioGraphics*, *26*(suppl_1), S173-S189. https://doi.org/10.1148/rg.26si065513

Altman, D. G., & Bland, J. M. (1983). Measurement in Medicine: The Analysis of Method Comparison Studies. *The Statistician*, *32*(3), 307. https://doi.org/10.2307/2987937

Barajas, R. F., Chang, J. S., Segal, M. R., Parsa, A. T., McDermott, M. W., Berger, M. S., & Cha, S. (2009). Differentiation of Recurrent Glioblastoma Multiforme from Radiation Necrosis after External Beam Radiation Therapy with Dynamic Susceptibility- weighted Contrast-enhanced Perfusion MR Imaging, *253*(2), 11.

Benner, T., Heiland, S., Erb, G., Forsting, M., & Sartor, K. (1997). Accuracy of gamma-variate fits to concentration-time curves from dynamic susceptibility-contrast enhanced MRI: Influence of time resolution, maximal signal drop and signal-to-noise. *Magnetic Resonance Imaging*, *15*(3), 307-317. https://doi.org/10.1016/S0730-725X(96)00392-X

Bland, M. (2004). How can I decide the sample size for a study of agreement between two methods of measurement? Access https://www-users.york.ac.uk/~mb55/meas/sizemeth.htm

Bjornerud, A., Sorensen, A. G., Mouridsen, K., & Emblem, K. E. (2011). T1- and T2* -Dominant Extravasation Correction in DSC-MRI: Part I—Theoretical Considerations and Implications for Assessment of Tumor Hemodynamic Properties. *Journal of Cerebral Blood Flow & Metabolism*, *31*(10), 2041-2053. https://doi.org/10.1038/jcbfm.2011.52

Boxerman, J. L., Prah, D. E., Paulson, E. S., Machan, J. T., Bedekar, D., & Schmainda, K. M. (2012). The Role of Preload and Leakage Correction in Gadolinium-Based Cerebral Blood Volume Estimation Determined by Comparison with MION as a Criterion Standard. *American Journal of Neuroradiology*, *33*(6), 1081-1087. https://doi.org/10.3174/ajnr.A2934

Boxerman, J. L., Schmainda, K. M., & Weisskoff, R. M. (2006). Relative Cerebral Blood Volume Maps Corrected for Contrast Agent Extravasation Significantly Correlate with Glioma Tumor Grade, Whereas Uncorrected Maps Do Not. *American Journal of Neuroradiology*, *27*, 859-867.

Bulakbasi, N., Kocaoglu, M., Farzaliyev, A., Tayfun, C., Ucoz, T., & Somuncu, I. (2005). Assessment of diagnostic accuracy of perfusion MR imaging in primary and metastatic solitary malignant brain tumors. *AJNR. American Journal of Neuroradiology*, *26*(9), 2187-2199.

Christen, T., Ni, W., Qiu, D., Schmiedeskamp, H., Bammer, R., Moseley, M., & Zaharchuk, G. (2013). High-resolution cerebral blood volume imaging in humans using the blood pool contrast agent ferumoxytol: High Resolution CBV Maps in Humans Using USPIOs. *Magnetic Resonance in Medicine*, *70*(3), 705-710. https://doi.org/10.1002/mrm.24500

Curie, M. (1923). Pierre Curie. *Autobiographical Notes* (p.167). New York: McMillan Co. Access http://web.archive.org/web/20110111211010/http://etext.lib.virginia.edu/etcbin/toccer-new2?id=CurPier.sgm&images=images/modeng&data=/texts/english/modeng/parsed&tag=public&part=2&division=div1

Davenport, R. (1983). The derivation of the gamma-variate relationship for tracer dilution curves. *Journal of Nuclear Medicine: Official Publication, Society of Nuclear Medicine*, *24*(10), 945-948.

Donahue, K. M., Krouwer, H. G. J., Rand, S. D., Pathak, A. P., Marszalkowski, C. S., Censky, S. C., & Prost, R. W. (2000). Utility of simultaneously acquired gradient-echo and spin-echo cerebral blood volume and morphology maps in brain tumor patients. *Magnetic Resonance in Medicine*, *43*(6), 845-853. https://doi.org/10.1002/1522-2594(200006)43:6<845::AID-MRM10>3.0.CO;2-J

Dong, X., Noorbakhsh, A., Hirshman, B. R., Zhou, T., Tang, J. A., Chang, D. C., … Chen, C. C. (2015). Survival trends of grade I, II, and III astrocytoma patients and associated clinical practice

patterns between 1999 and 2010: A SEER-based analysis. *Neuro-Oncology Practice*, npv016. https://doi.org/10.1093/nop/npv016

Emblem, K. E., Scheie, D., Due-Tonnessen, P., Nedregaard, B., Nome, T., Hald, J. K., … Bjornerud, A. (2008). Histogram Analysis of MR Imaging–Derived Cerebral Blood Volume Maps: Combined Glioma Grading and Identification of Low-Grade Oligodendroglial Subtypes. *American Journal of Neuroradiology*, *29*(9), 1664-1670. https://doi.org/10.3174/ajnr.A1182

Essock-Burns, E., Lupo, J. M., Cha, S., Polley, M.-Y., Butowski, N. A., Chang, S. M., & Nelson, S. J. (2011). Assessment of perfusion MRI-derived parameters in evaluating and predicting response to antiangiogenic therapy in patients with newly diagnosed glioblastoma. *Neuro-Oncology*, *13*(1), 119-131. https://doi.org/10.1093/neuonc/noq143

Food and Drug Administration (FDA). (2016). *K152602 - Olea Medical*. Access https://www.accessdata.fda.gov/cdrh_docs/pdf15/K152602.pdf

Food and Drug Administration (FDA). (2016). *K162025 - Philips Medical Systems Nederlands B.V*. Access https://www.accessdata.fda.gov/cdrh_docs/pdf16/K162025.pdf

Gahramanov, S., Muldoon, L. L., Varallyay, C. G., Li, X., Kraemer, D. F., Fu, R., … Neuwelt, E. A. (2013). Pseudoprogression of Glioblastoma after Chemo- and Radiation Therapy: Diagnosis by Using Dynamic Susceptibility-weighted Contrast-enhanced Perfusion MR Imaging with Ferumoxytol versus Gadoteridol and Correlation with Survival. *Radiology*, *266*(3), 842-852. https://doi.org/10.1148/radiol.12111472

Hirai, T., Murakami, R., Nakamura, H., Kitajima, M., Fukuoka, H., Sasao, A., … Yamashita, Y. (2008). Prognostic Value of Perfusion MR Imaging of High-Grade Astrocytomas: Long-Term Follow-Up Study. *American Journal of Neuroradiology*, *29*(8), 1505-1510. https://doi.org/10.3174/ajnr.A1121

Hu, L. S., Baxter, L. C., Pinnaduwage, D. S., Paine, T. L., Karis, J. P., Feuerstein, B. G., … Heiserman, J. E. (2010). Optimized Preload Leakage-Correction Methods to Improve the Diagnostic Accuracy of Dynamic Susceptibility-Weighted Contrast-Enhanced Perfusion MR Imaging in Posttreatment Gliomas. *American Journal of Neuroradiology*, *31*(1), 40-48. https://doi.org/10.3174/ajnr.A1787

Hu, L. S., Baxter, L. C., Smith, K. A., Feuerstein, B. G., Karis, J. P., Eschbacher, J. M., … Heiserman, J. E. (2009). Relative Cerebral Blood Volume Values to Differentiate High-Grade Glioma Recurrence from Posttreatment Radiation Effect: Direct Correlation between Image-Guided Tissue Histopathology and Localized Dynamic Susceptibility-Weighted Contrast-Enhanced Perfusion MR Imaging Measurements. *American Journal of Neuroradiology*, *30*(3), 552-558. https://doi.org/10.3174/ajnr.A1377

Jenoudet, H., Jenoudet, B., Waysberg, A., Duparc, B., Ghorbal, Y. B., Fresnais, F., … Merzeau, C. (2007). La perfusion cérébrale en IRM dans l'approche diagnostic des tumeurs cérébrales. Résultats préliminaires d'une étude prospective sur six mois., 31.

Kraemer, T. (s.d.). MR Neuro Perfusion Leakage Correction.

Landis, J. R., & Koch, G. G. (1977). The Measurement of Observer Agreement for Categorical Data. *Biometrics*, *33*(1), 159. https://doi.org/10.2307/2529310

Law, M., Yang, S., Babb, J. S., Knopp, E. A., Golfinos, J. G., Zagzag, D., & Johnson, G. (2004). Comparison of cerebral blood volume and vascular permeability from dynamic susceptibility contrast-enhanced perfusion MR imaging with glioma grade. *AJNR. American Journal of Neuroradiology*, *25*(5), 746-755.

Law, M., Young, R. J., Babb, J. S., Peccerelli, N., Chheang, S., Gruber, M. L., … Johnson, G. (2008). Gliomas: Predicting Time to Progression or Survival with Cerebral Blood Volume

Measurements at Dynamic Susceptibility-weighted Contrast-enhanced Perfusion MR Imaging. *Radiology*, *247*(2), 490-498. https://doi.org/10.1148/radiol.2472070898

Lee, J., Koh, D., & Ong, C. N. (1989). Statistical evaluation of agreement between two methods for measuring a quantitative variable. *Computers in Biology and Medicine*, *19*(1), 61-70. https://doi.org/10.1016/0010-4825(89)90036-X

Leu, K., Boxerman, J. L., & Ellingson, B. M. (2017). Effects of MRI Protocol Parameters, Preload Injection Dose, Fractionation Strategies, and Leakage Correction Algorithms on the Fidelity of Dynamic-Susceptibility Contrast MRI Estimates of Relative Cerebral Blood Volume in Gliomas. *American Journal of Neuroradiology*, *38*(3), 478-484. https://doi.org/10.3174/ajnr.A5027

Louis, D. N., Perry, A., Reifenberger, G., von Deimling, A., Figarella-Branger, D., Cavenee, W. K., … Ellison, D. W. (2016). The 2016 World Health Organization Classification of Tumors of the Central Nervous System: a summary. *Acta Neuropathologica*, *131*(6), 803-820. https://doi.org/10.1007/s00401-016-1545-1

Maia, A. C. M., Malheiros, S. M. F., da Rocha, A. J., Stávale, J. N., Guimarães, I. F., Borges, L. R. R., … Ferraz, F. A. P. (2004). Stereotactic biopsy guidance in adults with supratentorial nonenhancing gliomas: role of perfusion-weighted magnetic resonance imaging. *Journal of Neurosurgery*, 970-976. https://doi.org/10.3171/jns.2004.101.6.0970

Martin Bland, J., & Altman, D. (1986). STATISTICAL METHODS FOR ASSESSING AGREEMENT BETWEEN TWO METHODS OF CLINICAL MEASUREMENT. *The Lancet*, *327*(8476), 307-310. https://doi.org/10.1016/S0140-6736(86)90837-8

Olea Medical. (2013). Perfusion model (used in MRI - DSC and CT).

Østergaard, L., Weisskoff, R. M., Chesler, D. A., Gyldensted, C., & Rosen, B. R. (1996). High resolution measurement of cerebral blood flow using intravascular tracer bolus passages. Part I:

Mathematical approach and statistical analysis. *Magnetic Resonance in Medicine*, *36*(5), 715-725. https://doi.org/10.1002/mrm.1910360510

Paulson, E. S., & Schmainda, K. M. (2008). Comparison of Dynamic Susceptibility-weighted Contrast-enhanced MR Methods: Recommendations for Measuring Relative Cerebral Blood Volume in Brain Tumors. *Radiology*, *249*(2), 601-613. https://doi.org/10.1148/radiol.2492071659

Peusens, H. (2016). MR Neuro Perfusion in ISP9

Pickens, D. R., Price, R. R., & Yankeelov, T. (2012). *Quantitative MRI in cancer*. Boca Raton, FL: CRC Press.

Thompson, H. K., Starmer, C. F., Whalen, R. E., & Mcintosh, H. D. (1964). Indicator Transit Time Considered as a Gamma Variate. *Circulation Research*, *14*(6), 502-515. https://doi.org/10.1161/01.RES.14.6.502

Ulmer, S., Helle, M., Jansen, O., Mehdorn, H. M., & Nabavi, A. (2009). Intraoperative dynamic susceptibility contrast weighted magnetic resonance imaging (iDSC-MRI) — Technical considerations and feasibility. *NeuroImage*, *45*(1), 38-43. https://doi.org/10.1016/j.neuroimage.2008.11.021

Vonken, E. P. A., & Viergever, M. A. (1999). Measurement of cerebral perfusion with dual-echo multi-slice quantitative dynamic susceptibility contrast MRI, 9.

Welker, K., Boxerman, J., Kalnin, A., Kaufmann, T., Shiroishi, M., Wintermark, M., & for the American Society of Functional Neuroradiology MR Perfusion Standards and Practice Subcommittee of the ASFNR Clinical Practice Committee. (2015). ASFNR Recommendations for Clinical Performance of MR Dynamic Susceptibility Contrast Perfusion Imaging of the Brain. *American Journal of Neuroradiology*, *36*(6), E41-E51. https://doi.org/10.3174/ajnr.A4341

Bibliography

Abdulla, S., Saada, J., Johnson, G., Jefferies, S., & Ajithkumar, T. (2015). Tumour progression or pseudoprogression? A review of post-treatment radiological appearances of glioblastoma. *Clinical Radiology*, *70*(11), 1299-1312. https://doi.org/10.1016/j.crad.2015.06.096

Barajas, R. F., & Cha, S. (2014). Benefits of dynamic susceptibility-weighted contrast-enhanced perfusion MRI for glioma diagnosis and therapy. *CNS Oncology*, *3*(6), 407-419. https://doi.org/10.2217/cns.14.44

Barbier, E. L., Lamalle, L., & Décorps, M. (2001). Methodology of brain perfusion imaging: Methodology of Brain Perfusion Imaging. *Journal of Magnetic Resonance Imaging*, *13*(4), 496-520. https://doi.org/10.1002/jmri.1073

Base de données publique des médicaments. (2018). *Gadovist 1.0 mmol/ml, solution injectable en seringue pré-remplie*. Access http://base-donnees-publique.medicaments.gouv.fr/affichageDoc.php?specid=62409751&typedoc=N

Bland, J.M., Altman, D.G. (1990). A note on the use of the intraclass correlation coefficient in the evaluation of agreement between two methods of measurement. *Computers in biology and medicine, 20*(5), 337-340.

Boxerman, Jerrold L., Rosen, B. R., & Weisskoff, R. M. (1997). Signal-to-noise analysis of cerebral blood volume maps from dynamic NMR imaging studies. *Journal of Magnetic Resonance Imaging*, *7*(3), 528-537. https://doi.org/10.1002/jmri.1880070313

Boxerman, J.L., Paulson, E. S., Prah, M. A., & Schmainda, K. M. (2013). The Effect of Pulse Sequence Parameters and Contrast Agent Dose on Percentage Signal Recovery in DSC-MRI: Implications for Clinical Applications. *American Journal of Neuroradiology*, *34*(7), 1364-1369. https://doi.org/10.3174/ajnr.A3477

Compendium. (2017). *Gadovist 1.0 sol inj*. Access https://compendium.ch/prod/gadovist-1-0-sol-inj/fr

Fussell, D., & Young, R. J. (2013). Role of MRI perfusion in improving the treatment of brain tumors. *Imaging in Medicine*, *5*(5), 407-426. https://doi.org/10.2217/iim.13.50

Gahramanov, S., Raslan, A. M., Muldoon, L. L., Hamilton, B. E., Rooney, W. D., Varallyay, C. G., … Neuwelt, E. A. (2011). Potential for Differentiation of Pseudoprogression From True Tumor Progression With Dynamic Susceptibility-Weighted Contrast-Enhanced Magnetic Resonance Imaging Using Ferumoxytol vs. Gadoteridol: A Pilot Study. *International Journal of Radiation Oncology*Biology*Physics*, *79*(2), 514-523. https://doi.org/10.1016/j.ijrobp.2009.10.072

Guo, B. J., Yang, Z. L., & Zhang, L. J. (2018). Gadolinium Deposition in Brain: Current Scientific Evidence and Future Perspectives. *Frontiers in Molecular Neuroscience*, *11*. https://doi.org/10.3389/fnmol.2018.00335

Hu, L. S., Kelm, Z., Korfiatis, P., Dueck, A. C., Elrod, C., Ellingson, B. M., … Erickson, B. J. (2015). Impact of Software Modeling on the Accuracy of Perfusion MRI in Glioma. *American Journal of Neuroradiology*, *36*(12), 2242-2249. https://doi.org/10.3174/ajnr.A4451

Knopp, E. A., Cha, S., Johnson, G., Mazumdar, A., Golfinos, J. G., Zagzag, D., … Kricheff, I. I. (1999). Glial Neoplasms: Dynamic Contrast-enhanced T2*-weighted MR Imaging. *Radiology*, *211*(3), 791-798. https://doi.org/10.1148/radiology.211.3.r99jn46791

Law, M., Oh, S., Johnson, G., Babb, J. S., Zagzag, D., Golfinos, J., & Kelly, P. J. (2006). Perfusion Magnetic Resonance Imaging Predicts Patient Outcome as an Adjunct to Histopathology: A Second Reference Standard in the Surgical and Nonsurgical Treatment of Low-grade Gliomas. *Neurosurgery*, *58*(6), 1009-1107. https://doi.org/10.1227/01.NEU.0000215944.81730.18

Le Bas, J. F., Grand, S., Krainik, A., Lefournier, V., Tropres, I., & Rémy, C. (2006). IRM de perfusion des tumeurs cérébrales. *Journal de Radiologie*, *87*(6), 807-821. https://doi.org/10.1016/S0221-0363(06)74089-6

Leu, K., Boxerman, J. L., & Ellingson, B. M. (2017). Effects of MRI Protocol Parameters, Preload Injection Dose, Fractionation Strategies, and Leakage Correction Algorithms on the Fidelity of Dynamic-Susceptibility Contrast MRI Estimates of Relative Cerebral Blood Volume in Gliomas. *American Journal of Neuroradiology*, *38*(3), 478-484. https://doi.org/10.3174/ajnr.A5027

Levin, J. M., Wald, L. L., Kaufman, M. J., Ross, M. H., Maas, L. C., & Renshaw, P. F. (1998). T1Effects in Sequential Dynamic Susceptibility Contrast Experiments. *Journal of Magnetic Resonance*, *130*(2), 292-295. https://doi.org/10.1006/jmre.1997.1317

Litov, M. (2012). *Réalisation d'un fantôme de flux pour le contrôle qualité en IRM*. Access https://www.utc.fr/tsibh/public/3abih/12/stage/litov/index.html#realis

Liu, H.-L., Wu, Y.-Y., Yang, W.-S., Chen, C.-F., Lim, K.-E., & Hsu, Y.-Y. (2011). Is Weisskoff model valid for the correction of contrast agent extravasation with combined T1 and T2∗ effects in dynamic susceptibility contrast MRI?: Contrast agent extravasation in DSC-MRI. *Medical Physics*, *38*(2), 802-809. https://doi.org/10.1118/1.3534197

McDonald, R. J., McDonald, J. S., Kallmes, D. F., Jentoft, M. E., Murray, D. L., Thielen, K. R., … Eckel, L. J. (2015). Intracranial Gadolinium Deposition after Contrast-enhanced MR Imaging. *Radiology*, *275*(3), 772-782. https://doi.org/10.1148/radiol.15150025

McGraw, K. O., & Wong, S. P. (1996). Forming inferences about some intraclass correlation coefficients. *Psychological Methods*, *1*(1), 30-46. https://doi.org/10.1037/1082-989X.1.1.30

Morita, N., Wang, S., Chawla, S., Poptani, H., & Melhem, E. R. (2010). Dynamic susceptibility contrast perfusion weighted imaging in grading of nonenhancing astrocytomas. *Journal of Magnetic Resonance Imaging*, *32*(4), 803-808. https://doi.org/10.1002/jmri.22324

Olea Medical. (s.d.). Software User Guide: Olea Sphere ® 3.0. pp 165-171

Provenzale, J. M., Mukundan, S., & Barboriak, D. P. (2006). Diffusion-weighted and Perfusion MR Imaging for Brain Tumor Characterization and Assessment of Treatment Response. *Radiology*, *239*(3), 632-649. https://doi.org/10.1148/radiol.2393042031

Rasschaert, M., Emerit, A., Fretellier, N., Factor, C., Robert, P., Idée, J.-M., & Corot, C. (2018). Gadolinium Retention, Brain T1 Hyperintensity, and Endogenous Metals: A Comparative Study of Macrocyclic Versus Linear Gadolinium Chelates in Renally Sensitized Rats. *Investigative Radiology*, *53*(6), 328-337. https://doi.org/10.1097/RLI.0000000000000447

Schmainda, K. M., Rand, S. D., Joseph, A. M., Lund, R., Ward, B. D., Pathak, A. P., … Krouwer, H. G. J. (2004). Characterization of a first-pass gradient-echo spin-echo method to predict brain tumor grade and angiogenesis. *AJNR. American Journal of Neuroradiology*, *25*(9), 1524-1532.

Semmineh, N. B., Xu, J., Boxerman, J. L., Delaney, G. W., Cleary, P. W., Gore, J. C., & Quarles, C. C. (2014). An Efficient Computational Approach to Characterize DSC-MRI Signals Arising from Three-Dimensional Heterogeneous Tissue Structures. *PLoS ONE*, *9*(1), e84764. https://doi.org/10.1371/journal.pone.0084764

Société Canadienne du cancer. (2018). *Tumeurs au cerveau et à la moelle épinière*. Access http://www.cancer.ca/fr-ca/cancer-information/cancer-type/brain-spinal/brain-and-spinal-tumours/?region=on

Thompson, H. K., Starmer, C. F., Whalen, R. E., & Mcintosh, H. D. (1964). Indicator Transit Time Considered as a Gamma Variate. *Circulation Research*, *14*(6), 502-515. https://doi.org/10.1161/01.RES.14.6.502

Viallon, M., Cuvinciuc, V., Delattre, B., Merlini, L., Barnaure-Nachbar, I., Toso-Patel, S., … Haller, S. (2015). State-of-the-art MRI techniques in neuroradiology: principles, pitfalls, and clinical applications. *Neuroradiology*, *57*(5), 441-467. https://doi.org/10.1007/s00234-015-1500-1

Willats, L., & Calamante, F. (2013). The 39 steps: evading error and deciphering the secrets for accurate dynamic susceptibility contrast MRI: THE 39 STEPS: TOWARDS ACCURATE DSC-MRI. *NMR in Biomedicine*, *26*(8), 913-931. https://doi.org/10.1002/nbm.2833

Wintermark, M., Sesay, M., Barbier, E., Borbély, K., Dillon, W. P., Eastwood, J. D., … Yonas, H. (2005). Comparative Overview of Brain Perfusion Imaging Techniques. *Stroke*, *36*(9). https://doi.org/10.1161/01.STR.0000177884.72657.8b

Wu, Y., An, H., Krim, H., & Lin, W. (2007). An Independent Component Analysis Approach for Minimizing Effects of Recirculation in Dynamic Susceptibility Contrast Magnetic Resonance Imaging. *Journal of Cerebral Blood Flow & Metabolism*, *27*(3), 632-645. https://doi.org/10.1038/sj.jcbfm.9600374

Content of the exhibit

Figure 1 : Model free on Intellispace 19
Figure 2 : Gamma Variate on Intellispace 19
Figure 3 : Leakage correction on Intellispace 20
Figure 4 : Scatter plot inter-software between Intellispace and Olea 25
Figure 5 : Bland Altman inter-software between Intellispace and Olea 26
Figure 6 : Scatter plot between Intellispace and Olea with the 1st subgroup 27
Figure 7 : Scatter plot between Intellispace and Olea with the 2nd subgroup 28
Figure 8 : Scatter plot between Intellispace and Olea with the 3rd subgroup 29
Figure 9 : Patient n°88 on Intellispace and Olea 30
Figure 10 : Patient n°41 on Intellispace and Olea 31
Figure 11 : Scatter plot inter-operator between two trained users 32
Figure 12 : Bland Altman inter-operator between two trained users 32
Figure 13 : Patient n°11 with the two operators 33
Figure 14 : Patient n°39 with the two operators 34
Figure 15 : Scatter plot intra-software on Intellispace between leakage correction and gamma variate 35
Figure 16 : Bland Altman intra-software on Intellispace between leakage correction and gamma variate 35
Figure 17 : Patient n°63 with leakage correction and gamma variate 36
Figure 18 : Patient n°33 with leakage correction, gamma variate and morphologic T1- and T2-weighted imaging 37

Content of the tables

Table 1 : Angiogenesis diagnostic Intellispace versus Olea..... 26
Table 2 : Difference within the 3rd subgroup between Intellispace and Olea 29
Table 3 : rCBV of patient n°88 between Intellispace and Olea 30
Table 4 : rCBV of patient n°41 between Intellispace and Olea 31
Table 5 : rCBV of patient n°11 between the two operators..... 33
Table 6 : rCBV of patient n°39 between the two operators..... 34
Table 7 : rCBV of patient n°63 between leakage correction and gamma variate from Intellispace..... 36
Table 8 : Summary table of study's results with the three mains reproducibilities..... 38